

Avanzamenti e prospettive future delle tecniche e dei metodi di rivelazione per l'imaging in medicina nucleare



SAPIENZA
UNIVERSITÀ DI ROMA

Prof. Roberto Pani

Facoltà di Farmacia e Medicina - INFN Roma1

Dip. Medicina Molecolare Sapienza Università di Roma

What is emission tomography?

- Nuclear imaging techniques, based on the detection of photons in vivo, emitted by a radio-tracer injected into the patient.
- Diagnostic radiopharmaceuticals or tracers reflect physiological function with limited anatomical information

- Two different techniques:

- **Single Photon Emission Tomography (SPECT):**

- a tracer molecule is labelled with single γ -emitting radionuclides. (Tc99m)

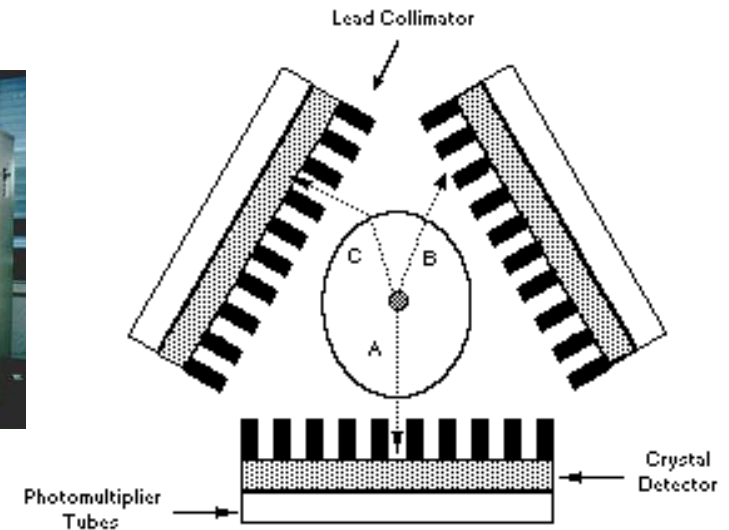
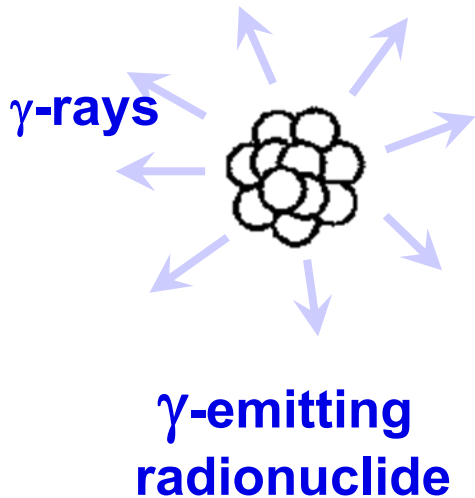
- **Positron Emission Tomography (PET):**

- a tracer molecule is labelled with positron-emitting radionuclides (18F, 11C).

SPET basic physics: single detection

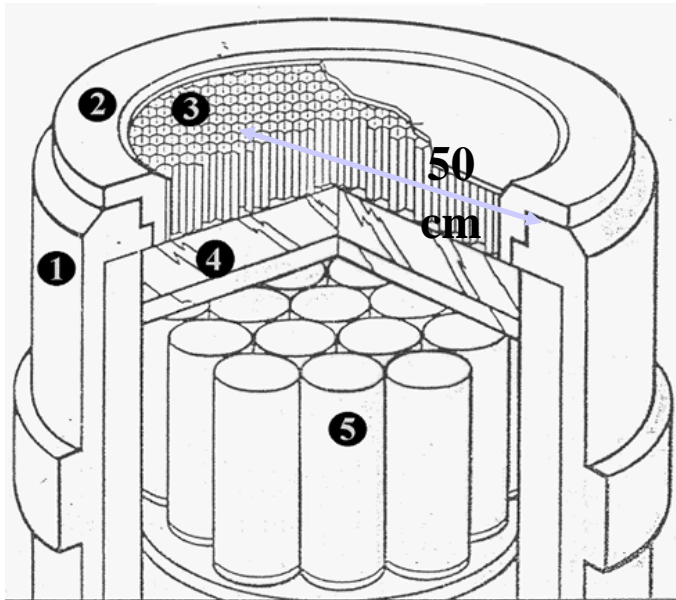
Most common nuclear imaging device (~ 22K units worldwide)

Single photon counting system Based upon NaI(Tl) scintillation detectors

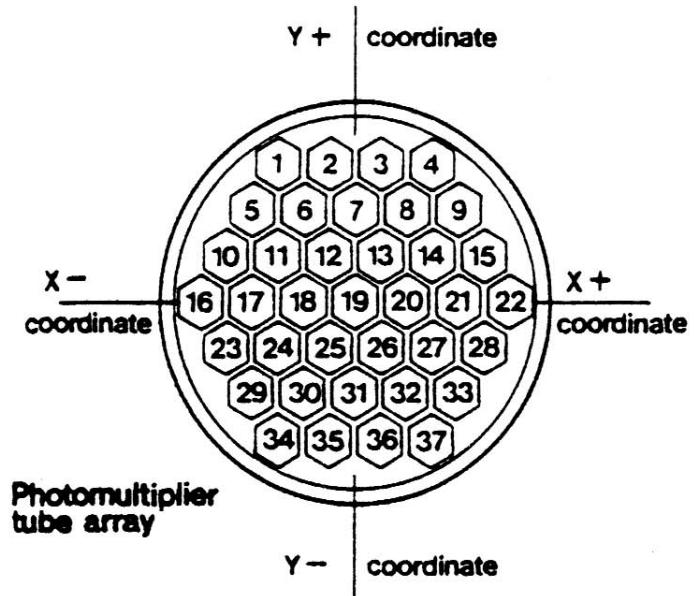


In contrast to PET scanners,
SPET radiation detectors typically rotate around the subject.

Imaging of Radio-isotopes : Anger Camera Basic



1. Housing
2. Lead shield
3. Collimator
4. NaI(Tl) crystal
5. PMTs

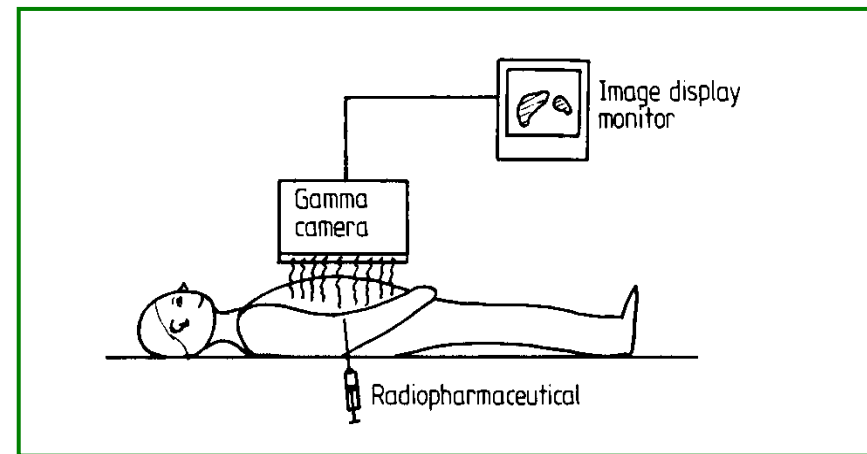


Four output signals

$$X = (x^+ - x^-) / (x^+ + x^-)$$

$$Y = (y^+ - y^-) / (y^+ + y^-)$$

Intrinsic Spatial Resolution ≈ 4 mm



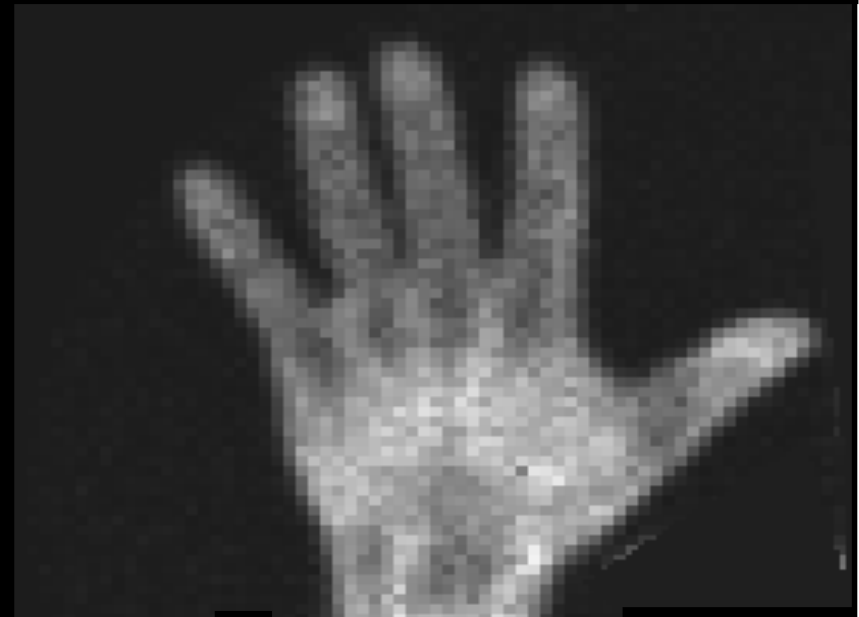
Relation To Anatomic Imaging

SPE Single Photon Emission

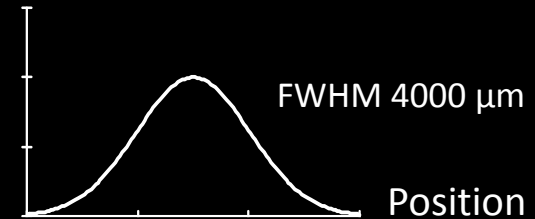
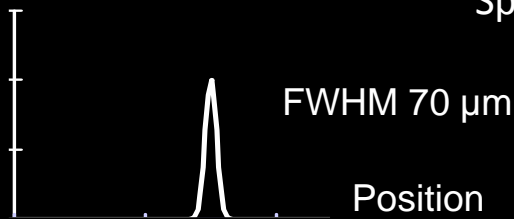
Anger Camera

^{99m}Tc MDP

RADIOLOGY X-RAY

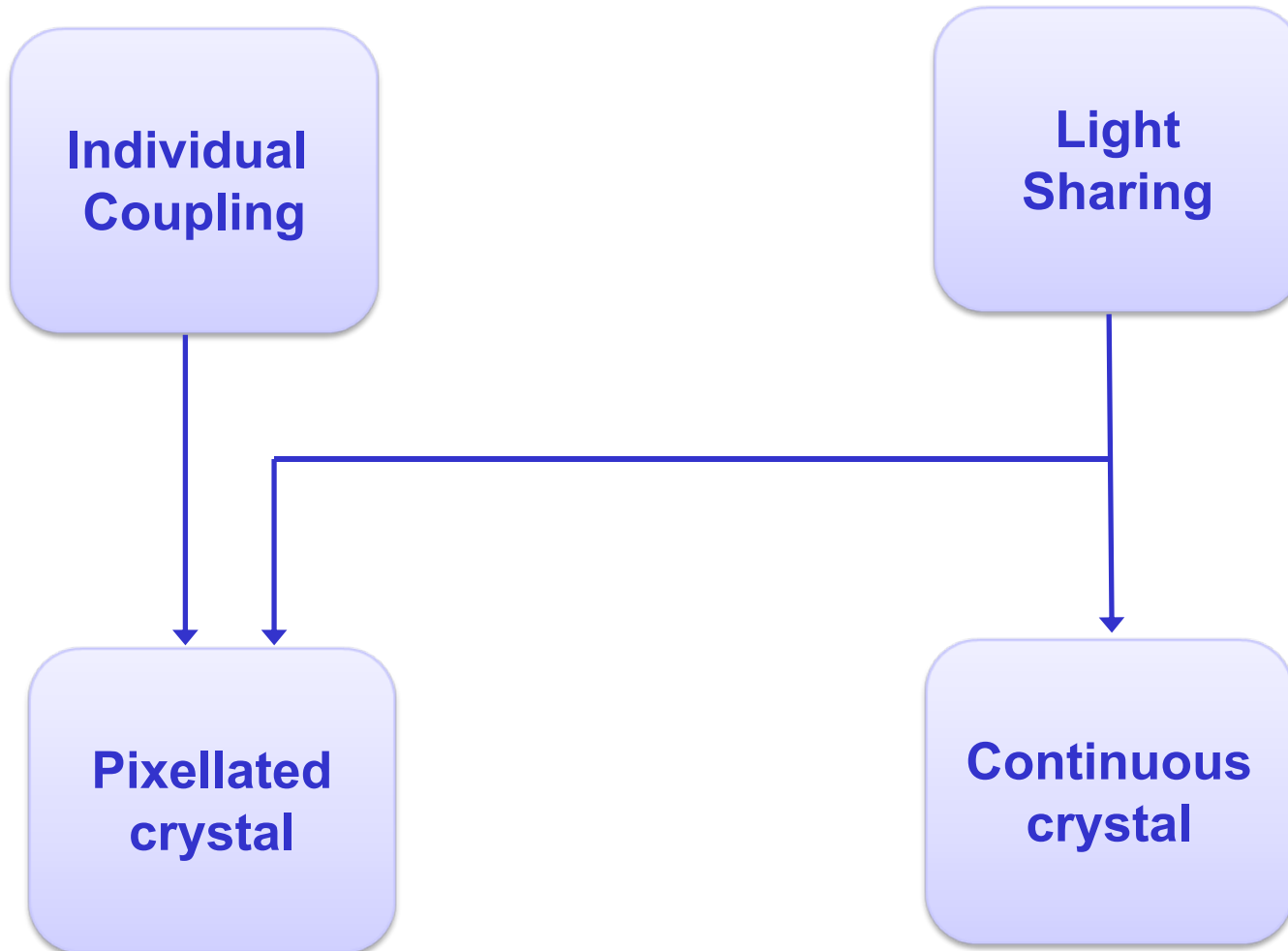


Spatial resolution



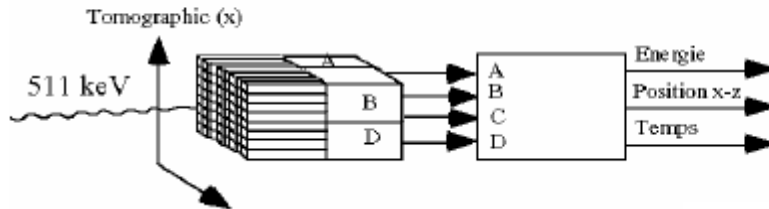
SPECT and PET detectors

Scintillation crystal read-out technique fall in the following categories



The most diffused PET Light Sharing: Block Detector

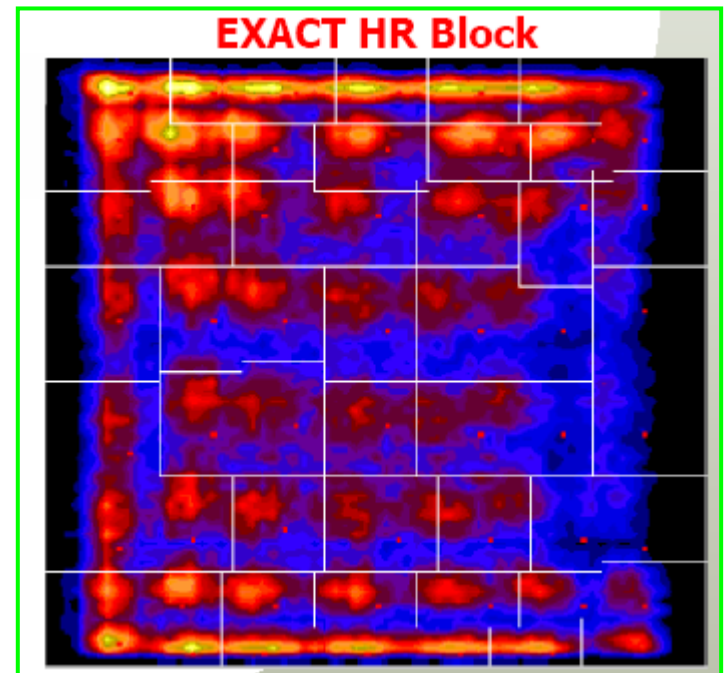
Casey & Nutt, *IEEE TNS* 33:460-3, 1986



$$x = \frac{(A+B) - (C+D)}{(A+B+C+D)}$$

$$z = \frac{(B+D) - (A+C)}{(A+B+C+D)}$$

- Array of (semi discrete detectors measured by 4 square PMTs
- Event positioning from light distribution probability map
- Crystal identification by look-up table
- Resolution loss due to
 - photon statistics
 - non linear positioning & distortion
 - pile-up at high rate



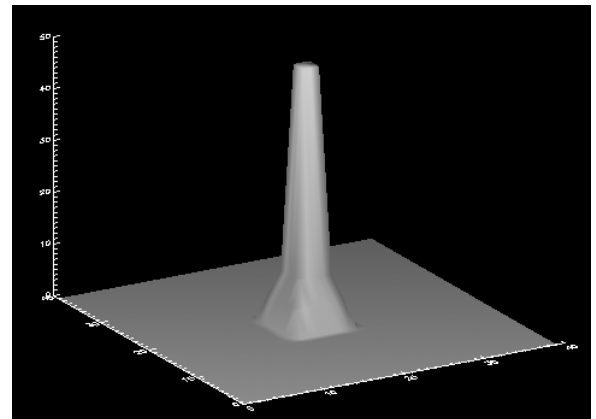
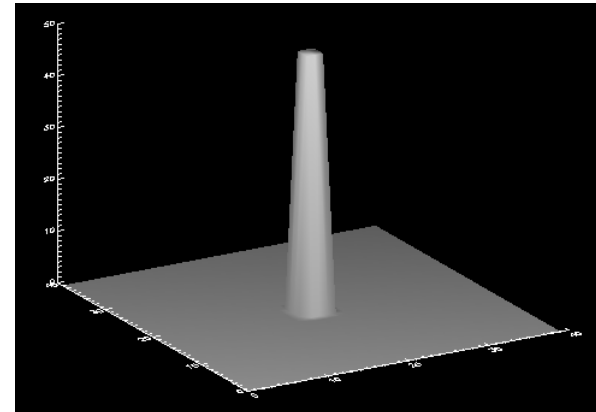
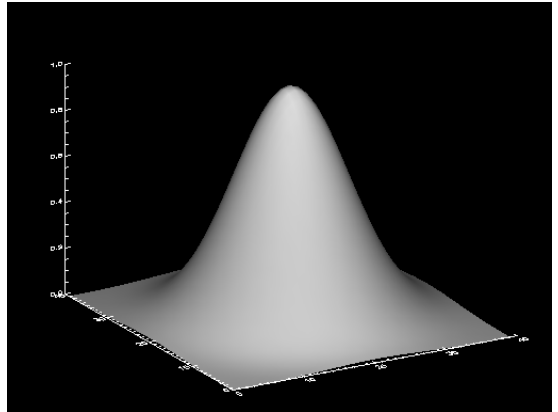
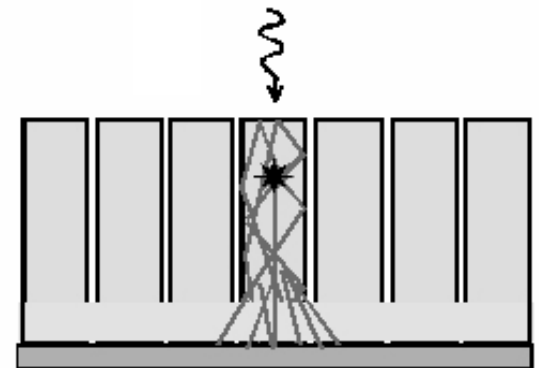
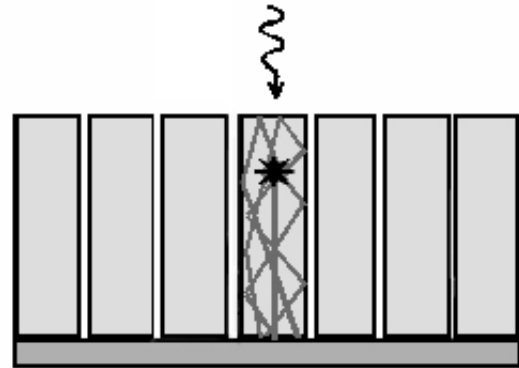
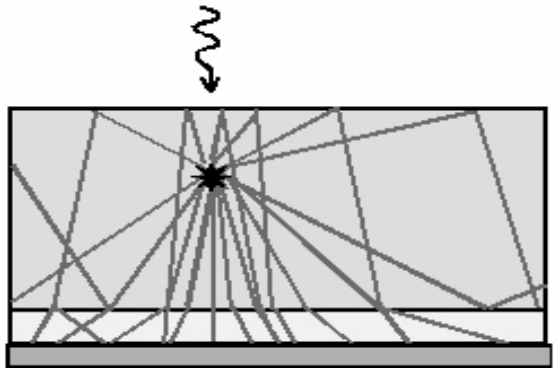
Courtesy of Roger Lecomte Sherbrooke University

Scintillation crystal read-out technique

Light Point Spread Function and critical angle θ_c

Continuos crystal / PMT glass window

Pixellated crystal / PMT glass window



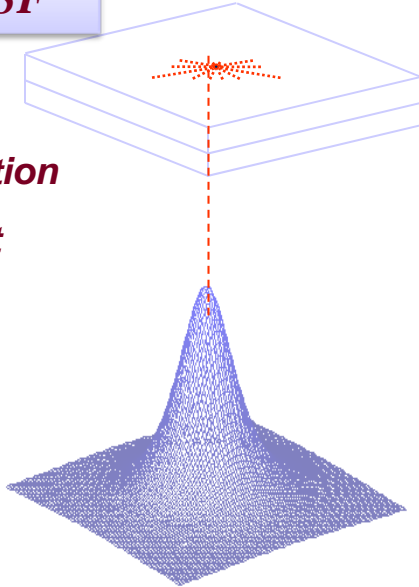
$$\theta_c = \text{sen}^{-1}\left(\frac{n_2}{n_0}\right) = 52^\circ$$

Light output angle $< 45^\circ$

**Position arithmetic and *intrinsic spatial resolution* by light sharing
Image and scintillation light PSF**

Light PSF

Scintillation event



$$X_c = \frac{\sum_j n_j x_j}{\sum_j n_j}$$

where

x_j represents the linear weight associated to the anode array

$$n_j = \sum_k n_{k,j}$$

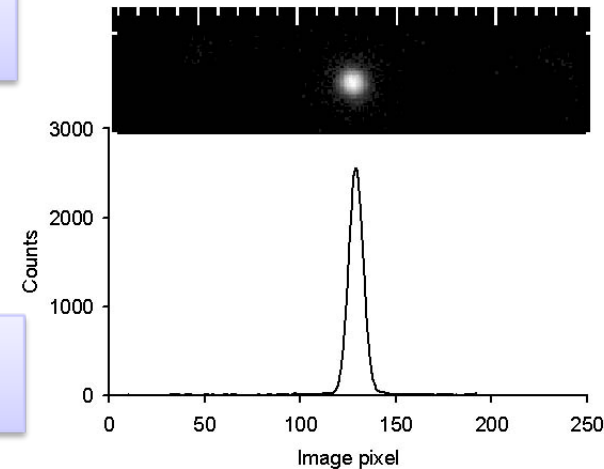
is the projection of the charge collected along the J-th column

Image PSF

$$\sigma_{imm} \approx \frac{\sigma_{PSF}}{\sqrt{n_{phe}}}$$

$$FWHM_{PSF_{image}} = 2.35 * \sigma_{X_c}$$

$$\sigma_{X_c}^2 = \sum_i \left(\frac{\partial X_c}{\partial n_i} \right)^2 \sigma_{n_i}^2$$



Spatial Resolution

$$SR = \frac{PSF_{imm}}{L}$$

$$L = \frac{dx_{measured}}{dx_{mech}}$$

L is ideally =1

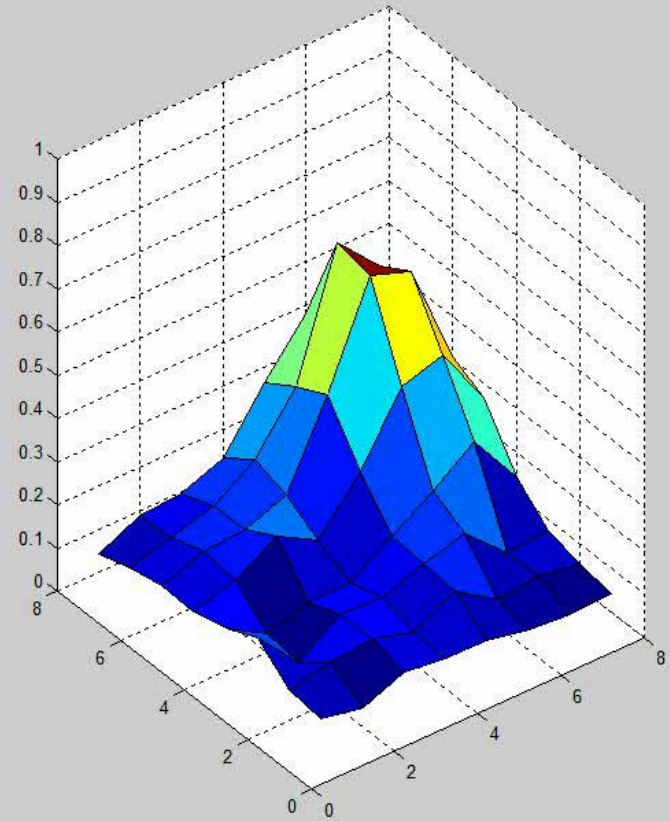
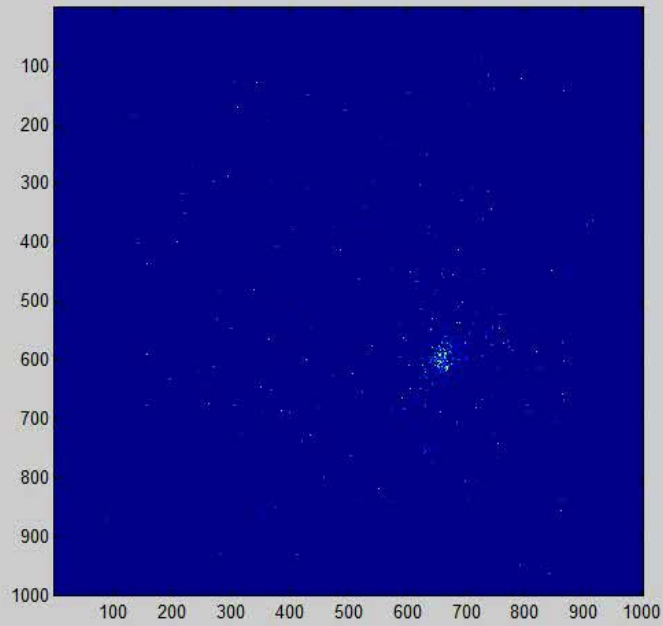


Image reconstruction of an irradiation spot (Tc^{99m})

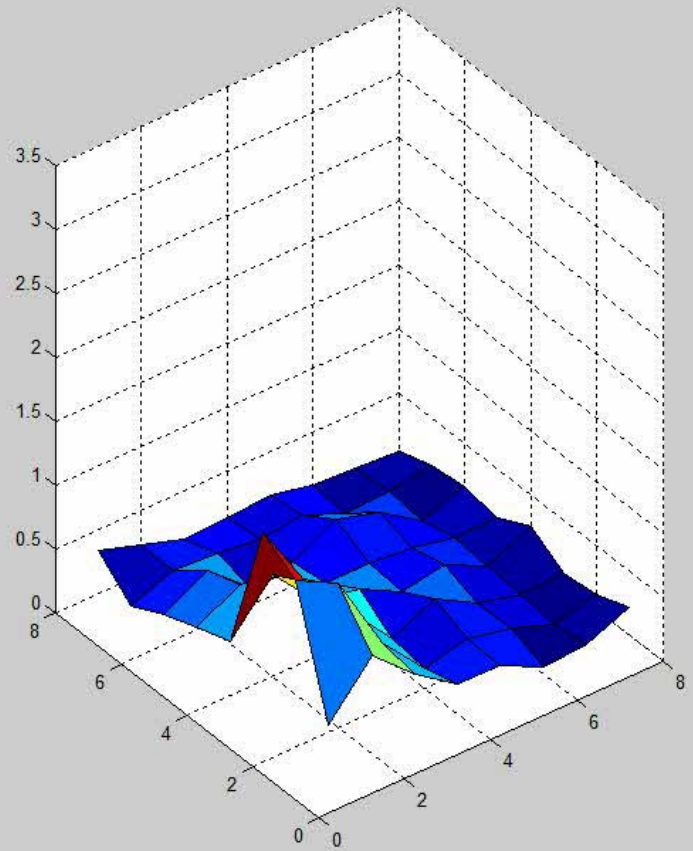
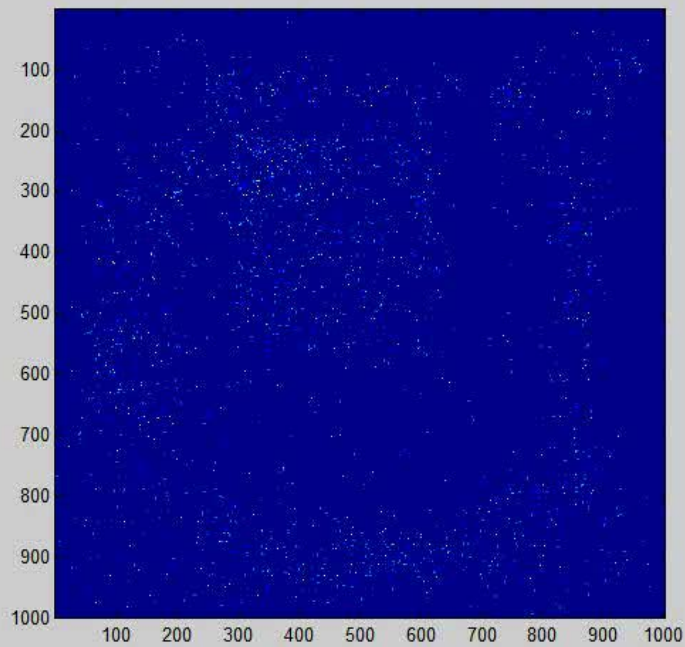
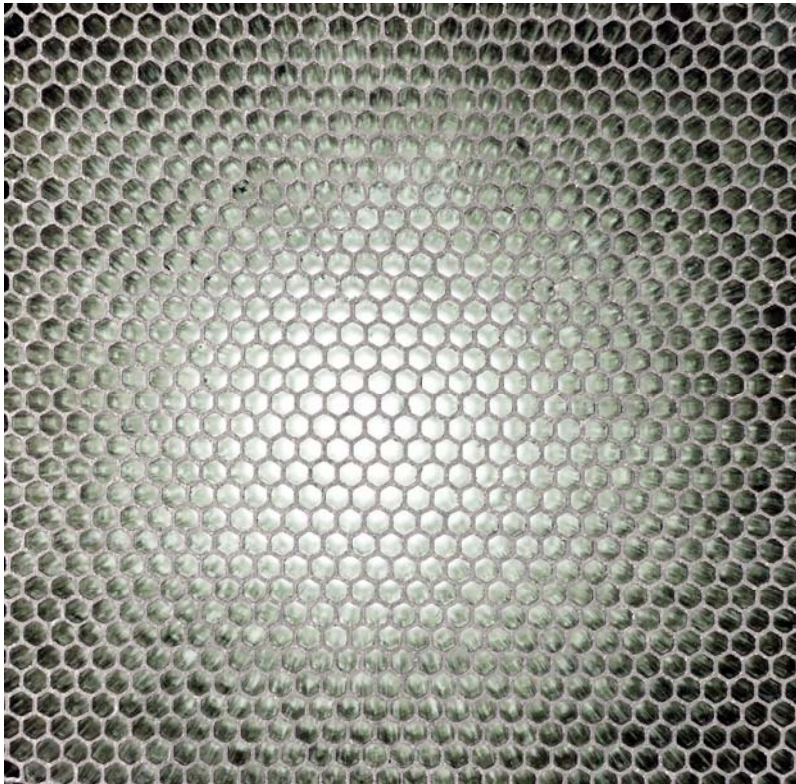


Image reconstruction of a collimator flood irradiation (Tc^{99m})

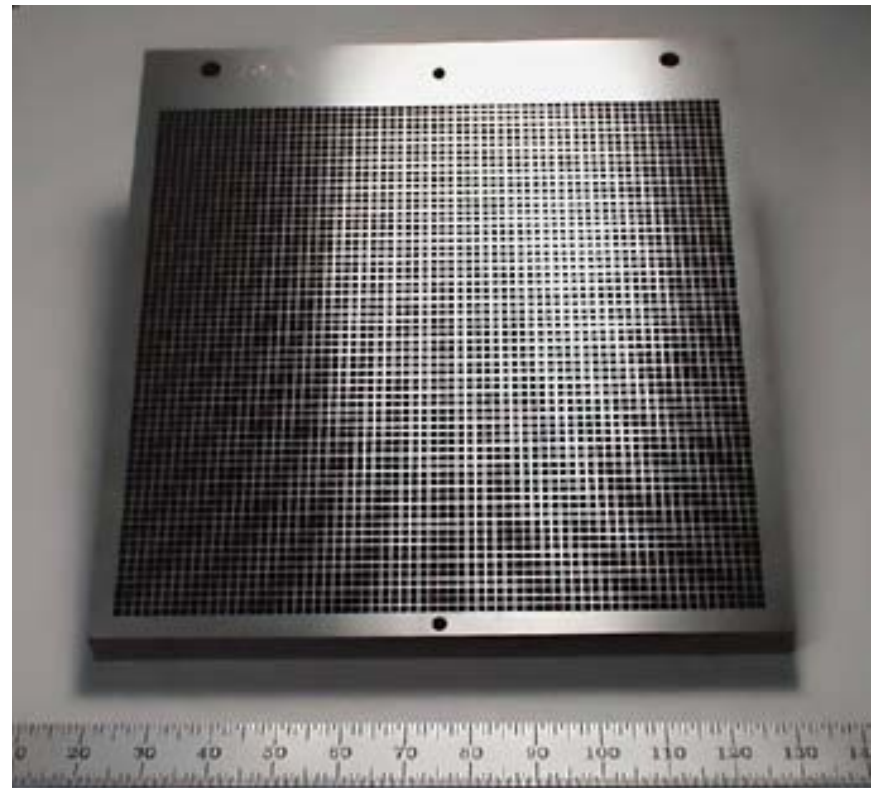
Example of Collimator Designs - Single Photon Imaging

Hexagonal-hole



Courtesy of Lawrence Berkeley Laboratory

Square-hole



Courtesy of Thermo Electron/Tecomet, Inc.

Collimator

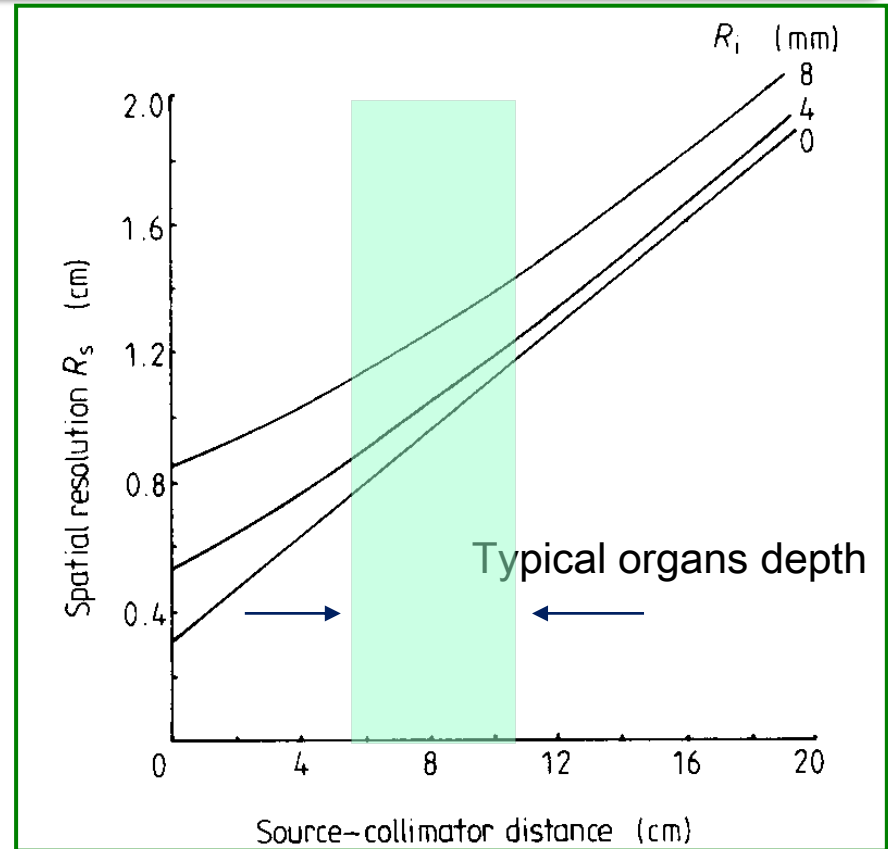
The major limitation of Sensitivity and Spatial Resolution

$$R_s = \sqrt{R_i^2 + R_c^2}$$

R_s = overall spatial resolution

R_i = intrinsic spatial resolution

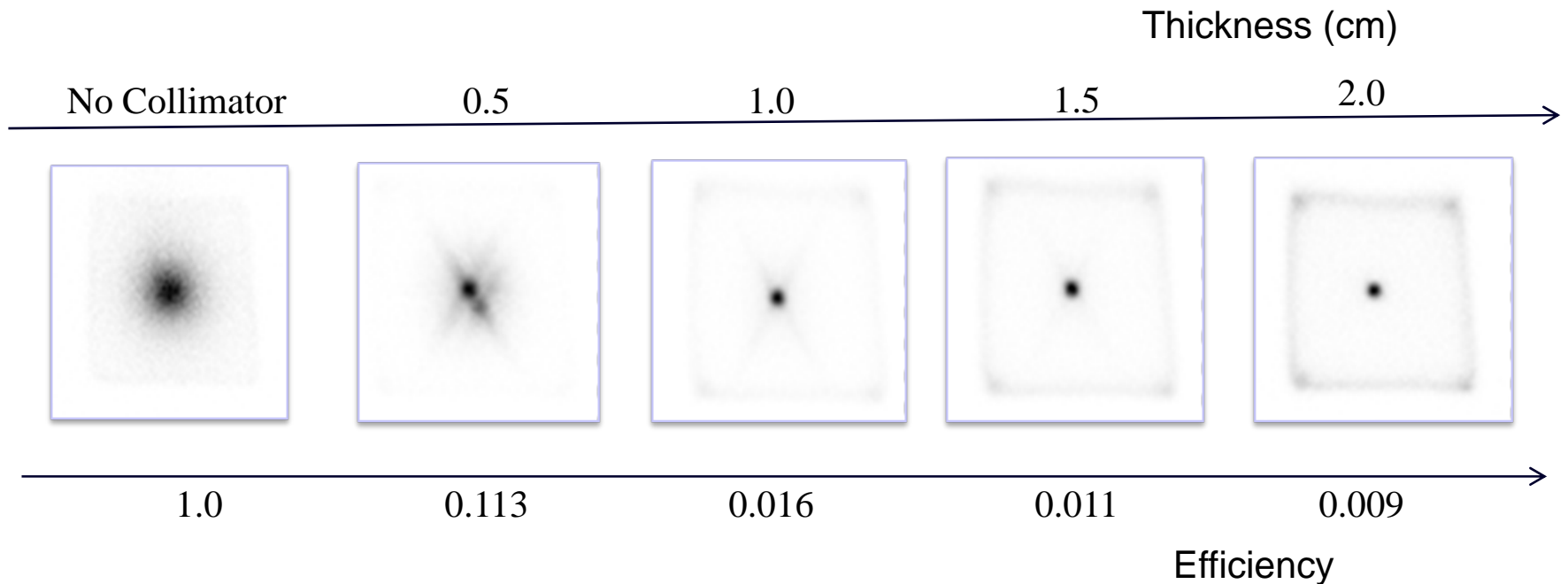
R_c = collimator resolution



Collimation	Spatial Resolution	Geometric Efficiency
Parallel-hole	degrades with source distance	constant with source distance

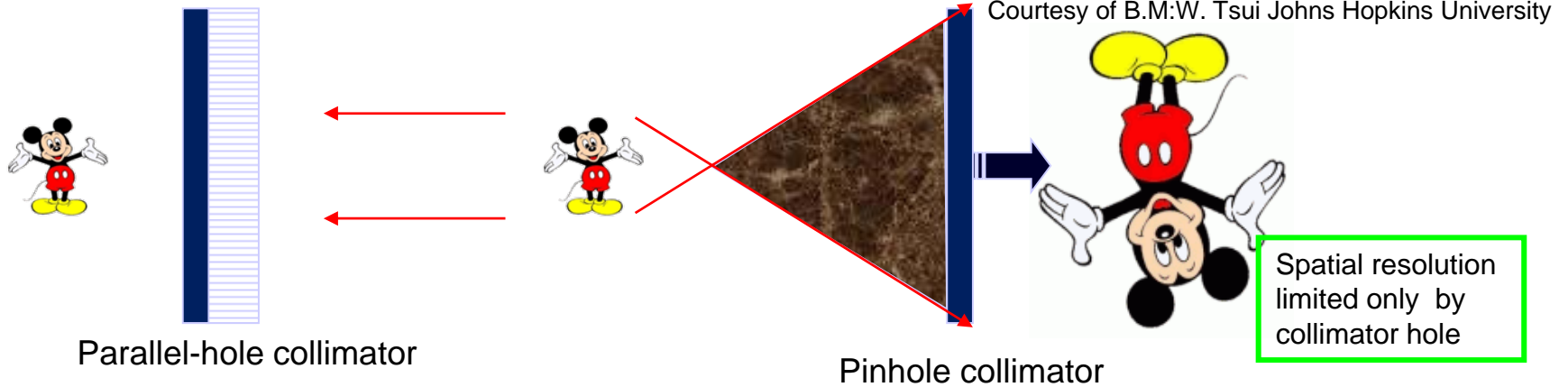
Reducing Collimator Thickness

Example: parallel-hole collimator on NaI(Tl)-PSPMT camera
Co-57 point source 1 cm from collimator

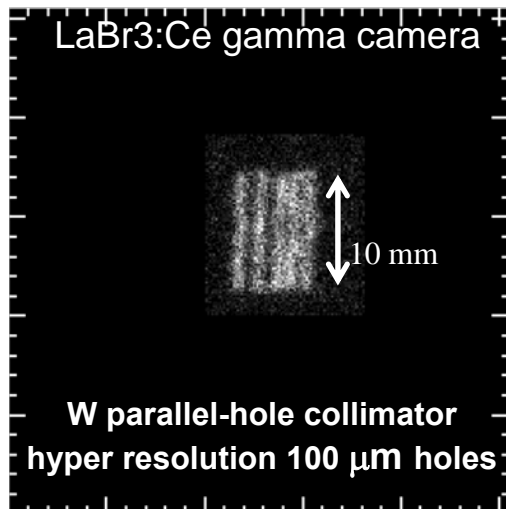


Courtesy of C.S. Levin UCSD school of Medicine USA

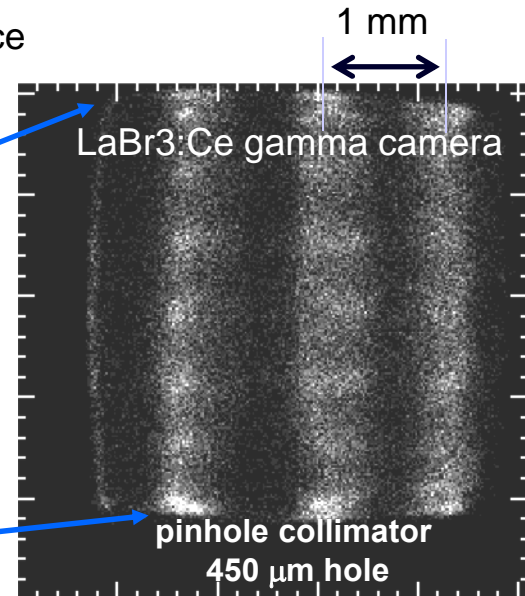
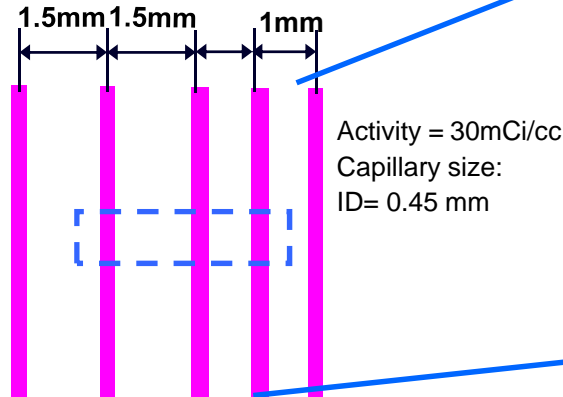
Parallel-Hole vs. Pinhole Collimation



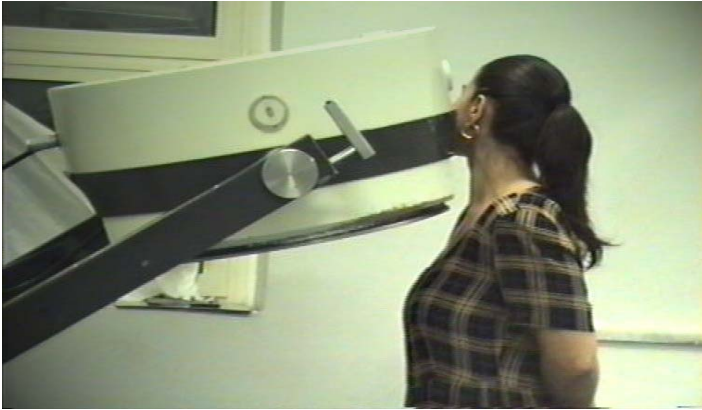
Spatial Resolution and Sensitivity degrades with source distance



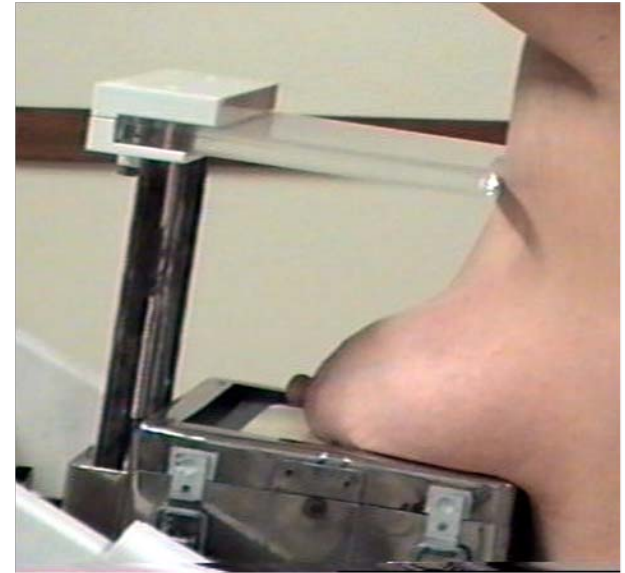
Capillary-setting source Tc^{99m}



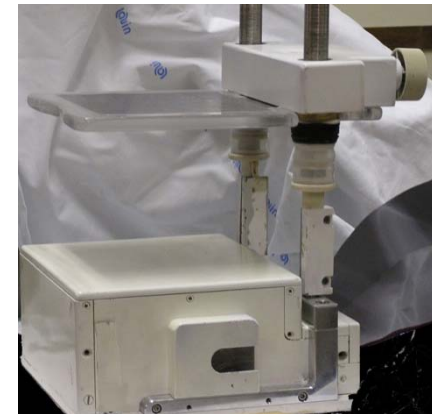
Motivation for the development of new cameras



Inability for close-proximity imaging
limited spatial resolution
limited sensitivity



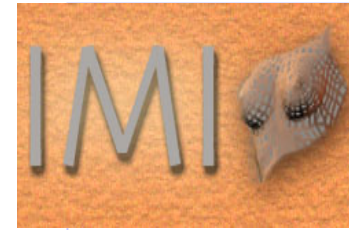
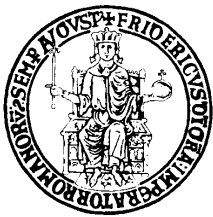
Scintimammography



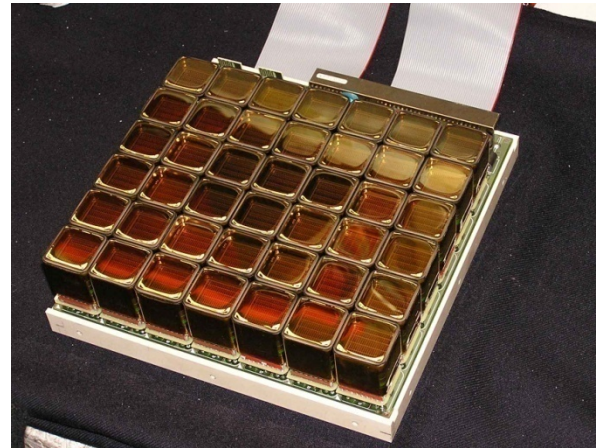
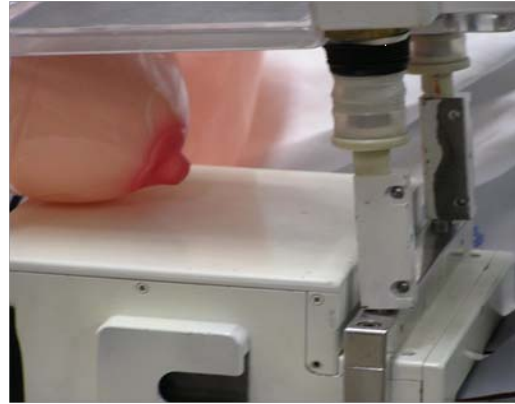
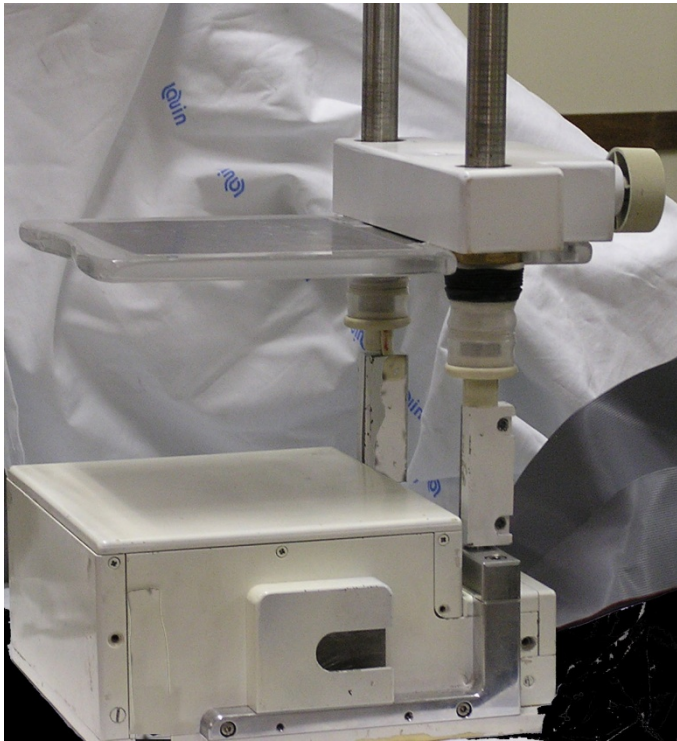
Dedicated gamma camera

Gamma camera dedicated to scintimammography

- *Detection ability of subcentimeter lesions*
- *Flexibility and accuracy of positioning at multiple orientations*
- *Close-proximity imaging*
- *Positioning at orientations to reduce background organ activity*
- *Incorporate into a mammography unit*
- *Mobile--can be taken into different clinical environments*
- *Design favoring very high spatial resolution at a reasonable cost*



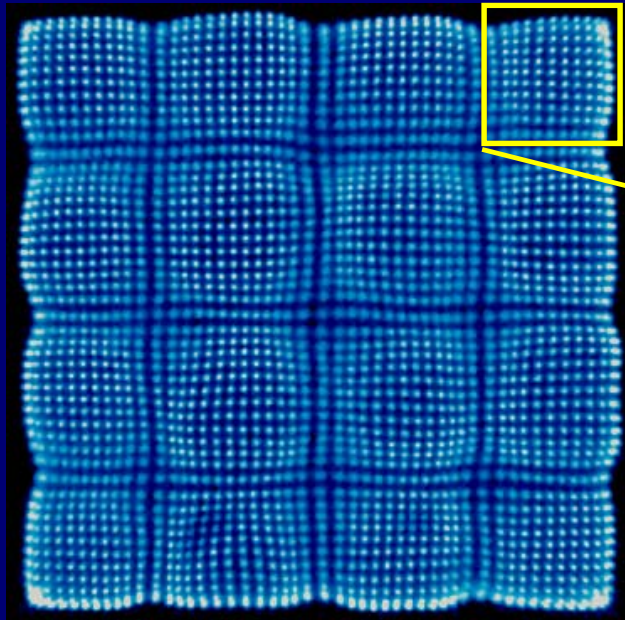
*1st Large FOV gamma camera based on INFN-“La Sapienza”
Photodetector design (Project IMI L46)*



Developed by Pol.Hi.Tech and CAEN

Image reconstruction from pixellated scintillation detector

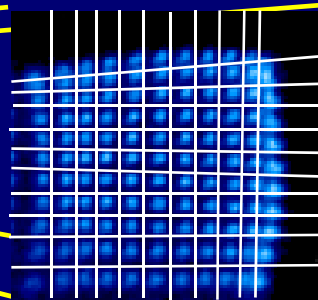
flood field image



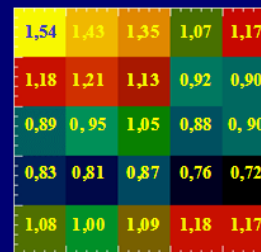
Integral uniformity = $\pm 16.9\%$

Differential uniformity = $\pm 4.5\%$

Intrinsic (pixel ID) spatial resolution = 0.9 ± 0.2 mm

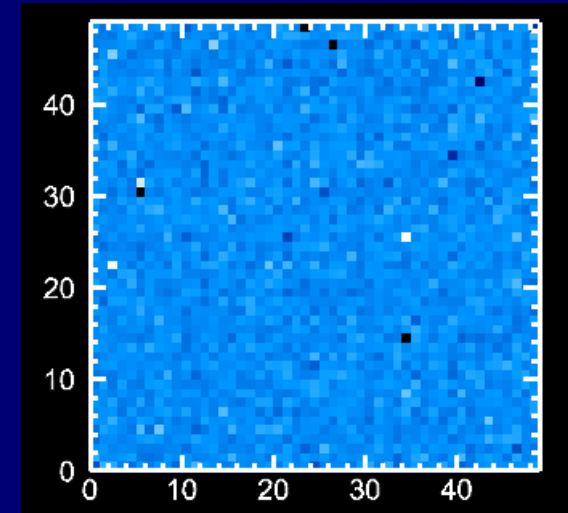


LUT pixels
spatial identification



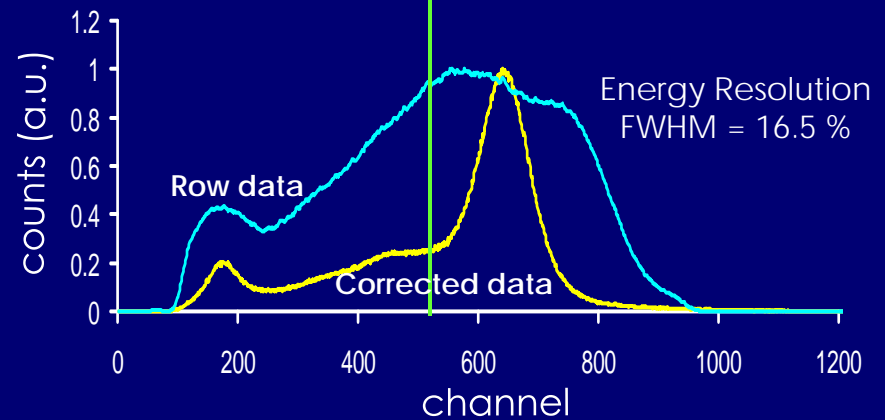
LUT cnts uniformity

LUT Reconstructed image



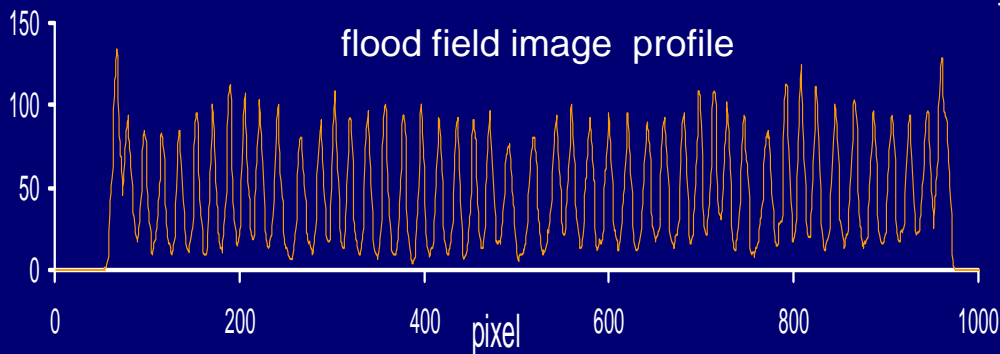
1.8 mm NaI (TI) pixel size

Photofraction = 63%



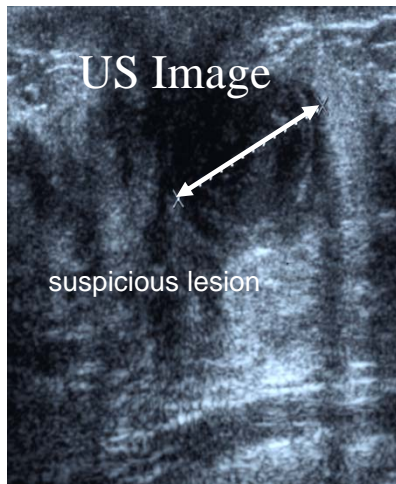
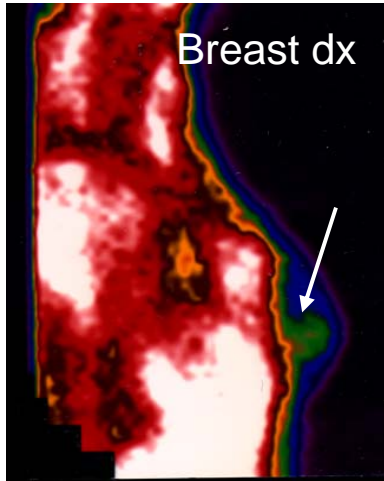
LUT pulse height distribution reconstruction

flood field image profile

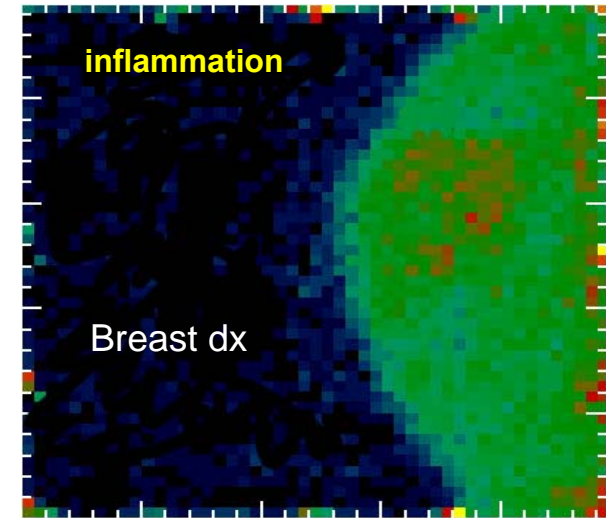
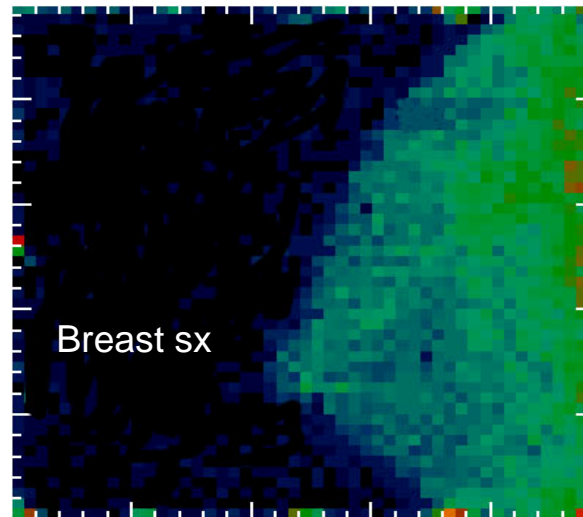


99mTc MIBI Scintimammography

Anger Camera



Dedicated gamma camera



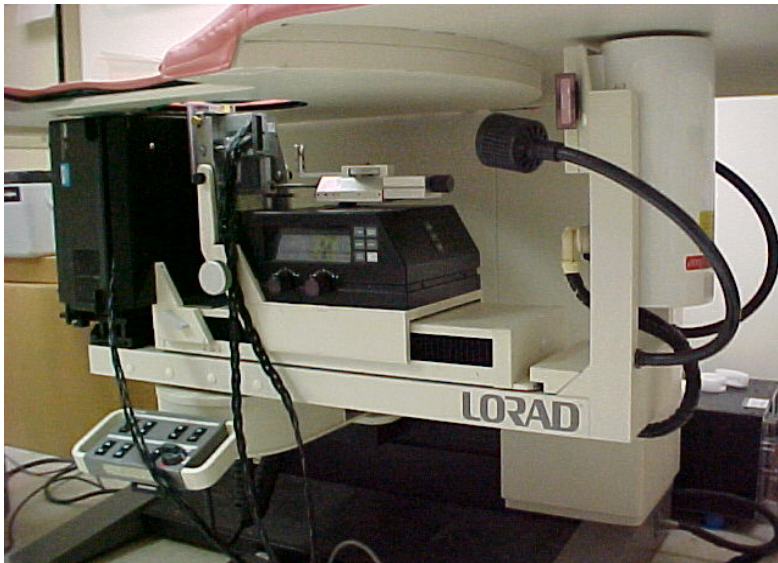
42 PSPMTs camera – NaI(Tl)

High Resolution Scintimammography helps in differentiating benign from malignant finding in scintigraphic hot spot

Application of PEM detectors

Combination Stereotactic Bx - PEM

Collaboration with PEM Technologies MA USA



- LORAD with PEM Detectors



- LORAD with patient and PEM Detectors

New Imaging Devices

Ultra High Resolution Small Animal Imaging

New PET scanners provide excellent sensitivity and spatial resolution of the order of 1-2 mm

Advanced SPET and PET scanners are currently under development

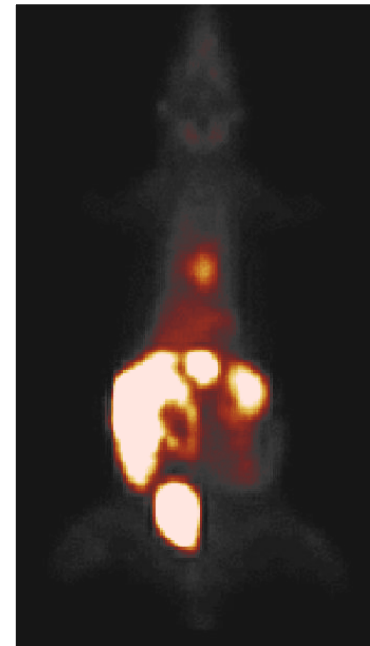
New SPET scanners provide ultra high spatial Resolution (1 mm or better) at the cost of low sensitivity and a reduced field of view.

Assessment of Myocardial Perfusion & Function Using ^{99m}Tc -Sestamibi in Rats & Mice

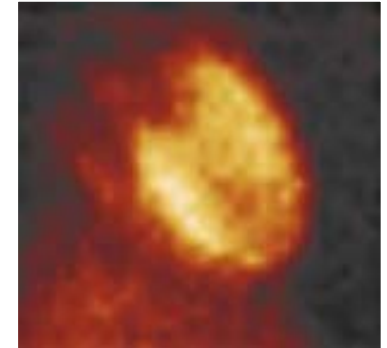
CsI (TI) Pixellated scintillation crystal

Experimental Animal Protocols:

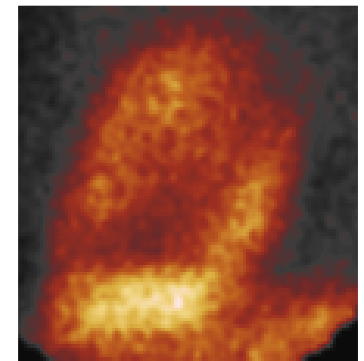
The performance of the prototype planar camera was evaluated for assessing myocardial perfusion and function using ^{99m}Tc - sestamibi (20 mCi) as well as inflammation following ischemia/reperfusion with the neutrophil tracer ^{99m}Tc -RP517 (2-20 mCi). 350 g male Sprague-Dawley rats and 20 g C57BL/6 mice were used in these experiments



Rat Whole Body
Clinical Gamma Camera



Rat Heart: static image



Mouse Heart: static image

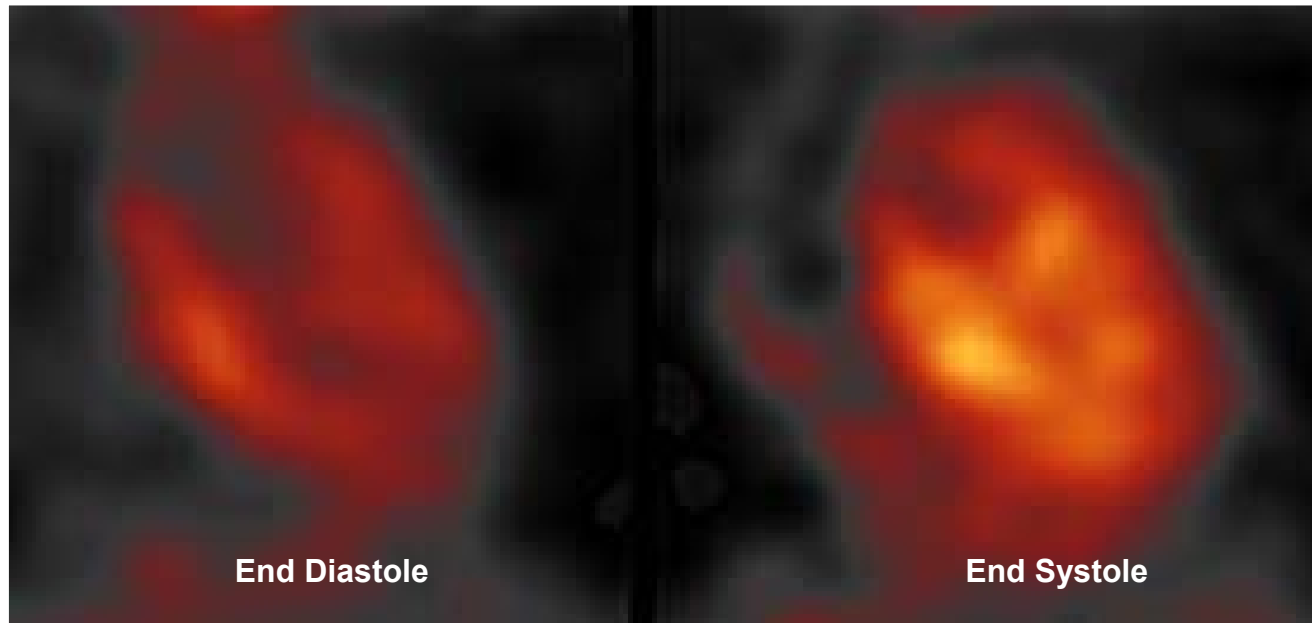
FAR LEFT: *In vivo* parallel hole static planar image of a rat using a standard clinical camera with high resolution, parallel-hole collimator. The resolution of standard clinical cameras is insufficient for imaging structural details in the hearts of small animals. NEAR LEFT: Rat and mouse *in vivo* static pinhole images acquired using the high resolution system. Note that the ventricular chambers and walls can be visualized.

Collaboration with University of Virginia Experimental Nuclear Cardiology Laboratory, and Detector Group, Thomas Jefferson National Accelerator Facility USA

In vivo gated planar image of the heart

*Collaboration with University of Virginia Experimental Nuclear
Cardiology Laboratory, and Detector Group, Thomas Jefferson National
Accelerator Facility USA*

*Pixellated scintillation crystal
Pinhole collimator*



In vivo gated planar image of a rat using a 1 mm pinhole. The left image shows the heart at the end diastolic or filled phase, and the right image shows the heart at the end systolic or empty phase of the cardiac cycle.

Latest Technological Advances

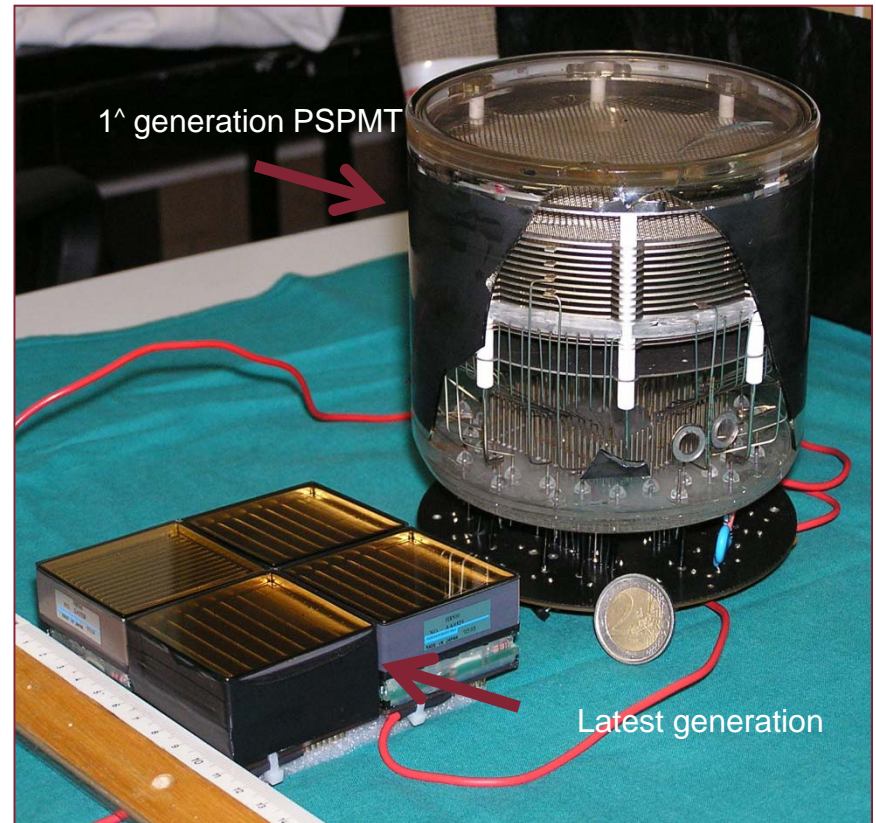
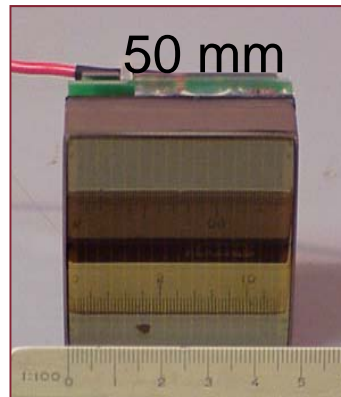
Hamamatsu H8500 segmented PMT (MAPMT) 38% QE

Gamma Camera Module

Photodetector: Position sensitive Flat Panel PMT H8500 Hamamatsu

- Extremely compact (15 mm of thickness)
- Ideal for closely packing in array (1.5 mm edge dead zone)
- Intrinsic spatial resolution better than 0.5 mm

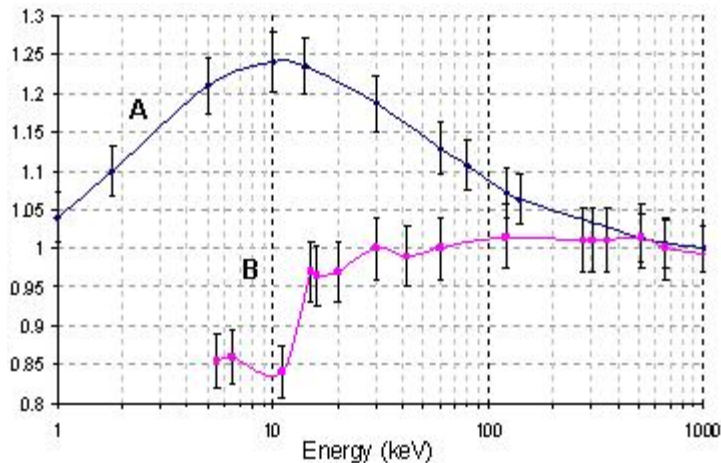
It allows large detection area modules for compact SPET system



LaBr₃:Ce : latest generation of scintillation crystals

	E (keV)	Density (g/cm ³)	Atten.len. (mm)	Z _{eff}	Photo-fraction (%)	Light yield (ph/MeV)	Decay time (ns)	Refr. index	ΔE/E (PMT)	Emiss max (nm)
CsI(Tl)	140	4.51	2.55	52.0	86	66,000	630	1.80	14%	565
LaBr ₃ :Ce	140	5.07	3.32	47.4	79	63,000	16 (97%)	1.90	6%	380
NaI:Tl	140	3.67	3.76	51.0	84	38,000	230	1.85	9%	410

Light Yield vs Energy



A – Prescott and Narayan, NIM A, 75 (1969)

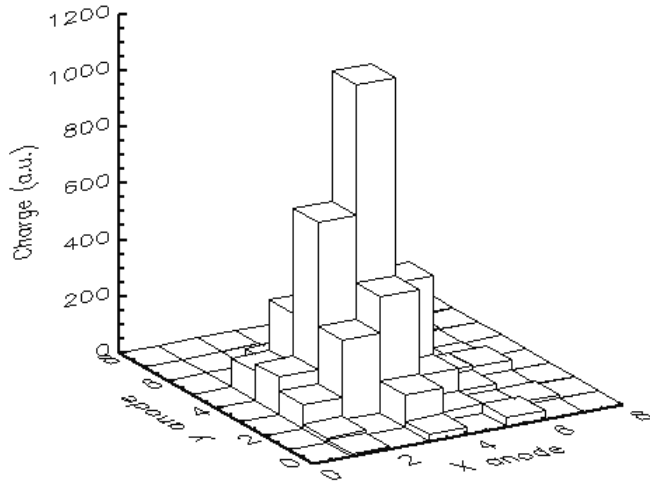
B – G. Bizarri, IEEE TNS, Vol 53,02 (2006)

Energy Resolution

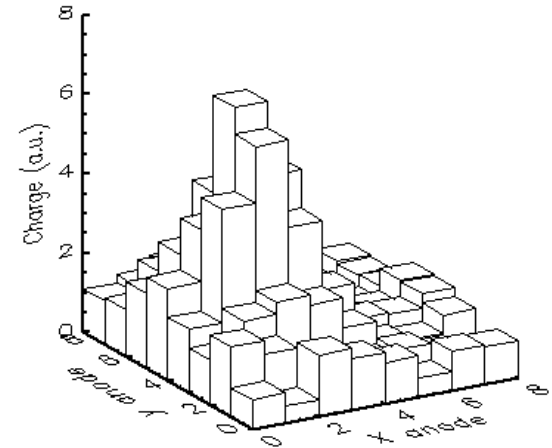
$$R^2(E) = R_s^2 + \frac{5.56}{N\eta\alpha} \left(\frac{\delta}{\delta - 1} \right)$$

Crystal	ER(%) @ 662 keV	ER _{scint.} (%)	ER _{st} (%)	Ref.
NaI(Tl)	6.7	5.9	3.2	typical
CsI(Tl)	6.6	5.8	3.2	Allier (1998)
LaBr ₃ (Ce)	3.6	2.2	2.5	Moszynski (2006)

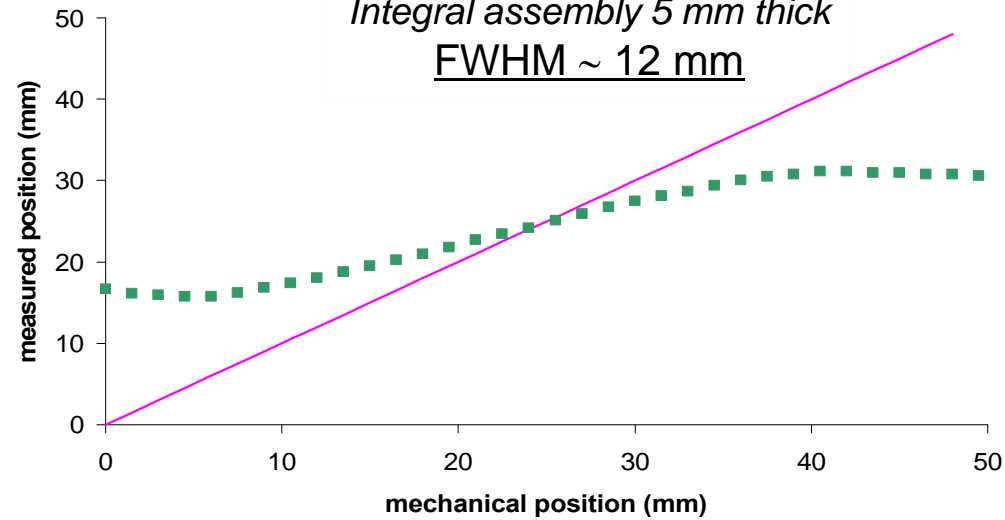
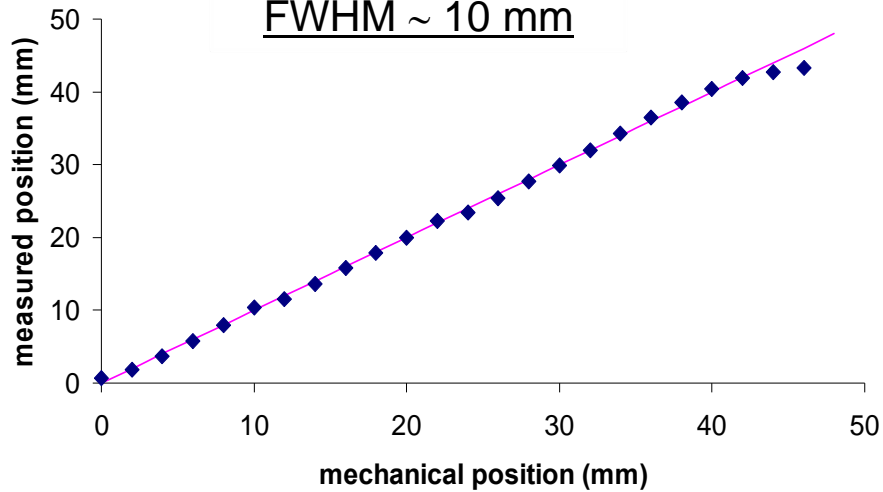
Ideal Position linearity of Scintillation array



NaI:TI 24x24 array
1.8 x 1.8 x 6 mm³ pixel
FWHM ~ 10 mm



LaBr₃:Ce
Integral assembly 5 mm thick
FWHM ~ 12 mm



New position arithmetic for continuous Scintillators based on floating weights

$$X_C = \frac{\sum_j n_j x_j}{\sum_j n_j}$$

where

represents the linear weight associated to the anode array x_j

$$n_j = \sum_k n_{k,j}$$

is the projection of the charge collected along the J-th column

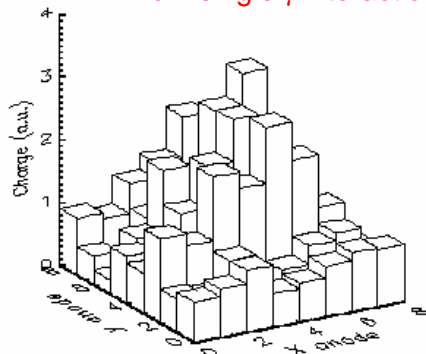
New algorithm:

$$X_C = \frac{\sum_j n'_j x_j}{\sum_j n'_j} \text{ where } n'_j = \sum_k (n_{k,j} \cdot w_{k,j});$$

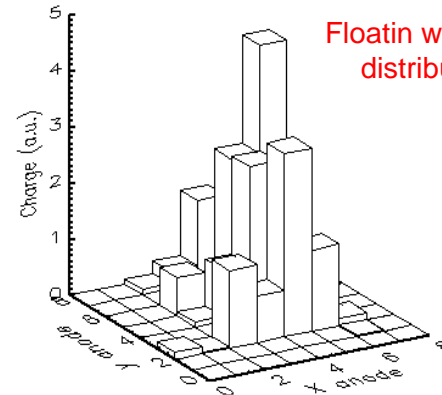
$w_{k,j} = n_{k,j}$ is the weight.

In general $w_{k,j}$ is a 2D array of weights strictly related to $n_{k,j}$. In this way the position information related to the anode position x_j is more *enhanced near the interaction point* (*maximum charge = maximum weight*) and depressed far from interaction location.

Original charge distribution from single γ interaction



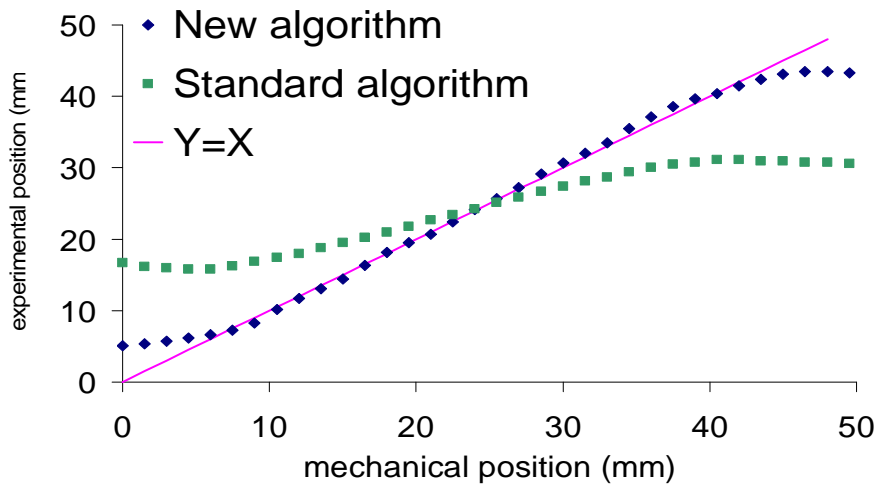
Floatin weighted distribution



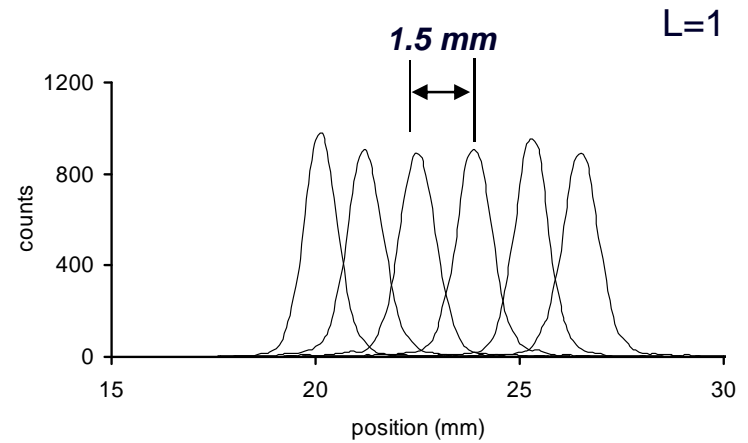
New position arithmetic

LaBr₃:Ce 5 mm thick (integral assembly)
Tc99m scanning 0.4mm coll

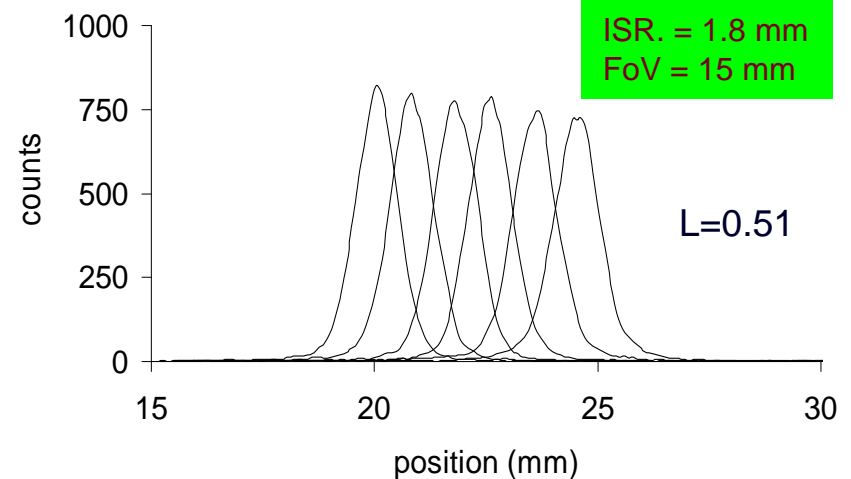
$$L = \frac{dX_{measured}}{dx_{mech}} = 0.51$$



ISR. = 0.9 ÷ 1.0 mm
FoV = 38 mm



Central Spots



Continuous crystal

can solve limitations offered by segmented detectors

^{99m}Tc Flood Field
Absorption image

Lead test object



^{99m}Tc FLAT FIELD
GEOMETRY

SOURCE
 $\text{Tc } ^{99m}$

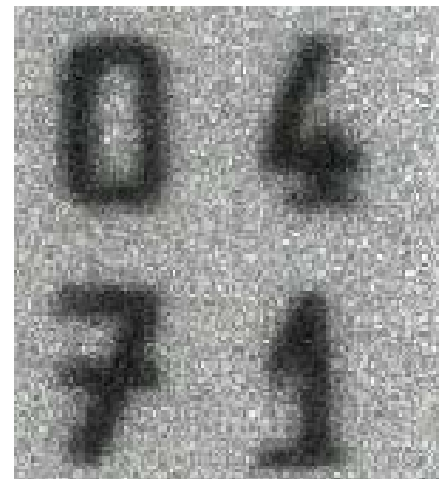
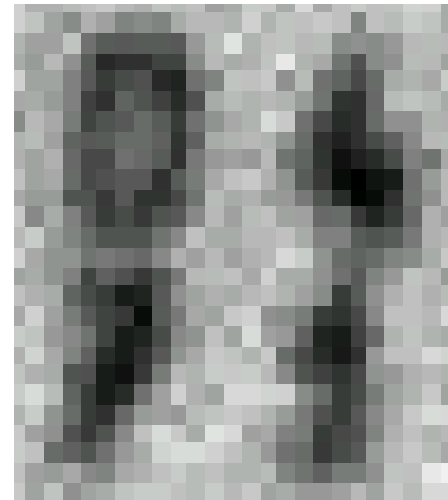


$\text{LaBr}_3:\text{Ce}$ 5 mm thick



CsI(Tl)-R2486
 $1 \times 1 \times 3 \text{ mm}^3$ pixel size

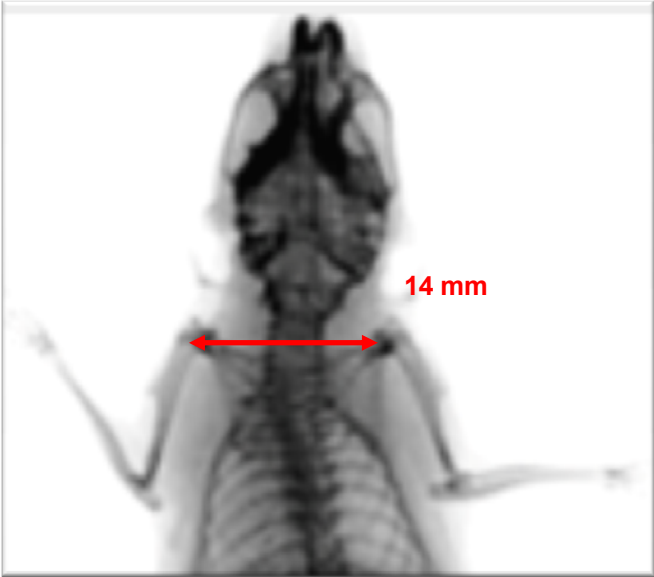
NaI:Tl – Anger camera



YAP:Ce
 $0.5 \times 0.5 \times 10 \text{ mm}^3$ pixel size

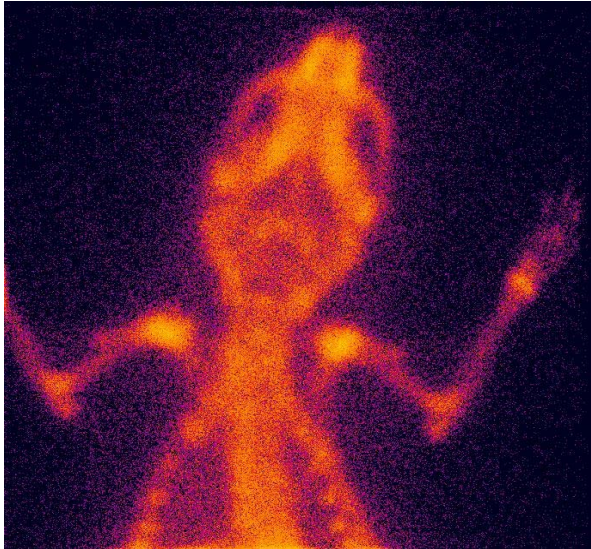
*Continuous vs Pixellated crystal
Mouse injected with ^{99m}Tc MDP*

X ray image



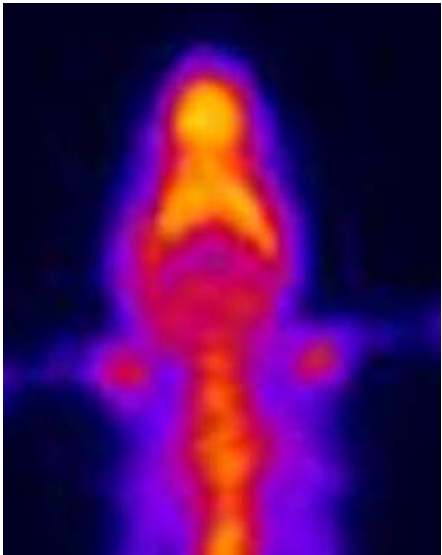
*1 mm continuous NaI(Tl)
H9500 MA-PMT*

*Parallel Hole Collimator
(0.364 mm hole, 0.105 mm
septa, 10.6 mm length)*

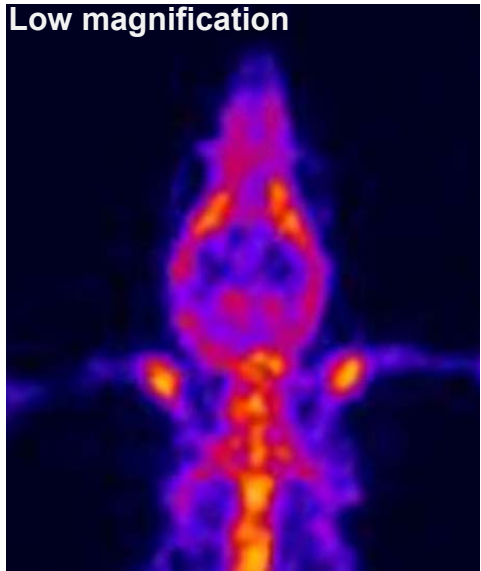


Courtesy of JLAB, Virginia, USA -S.Majewsky

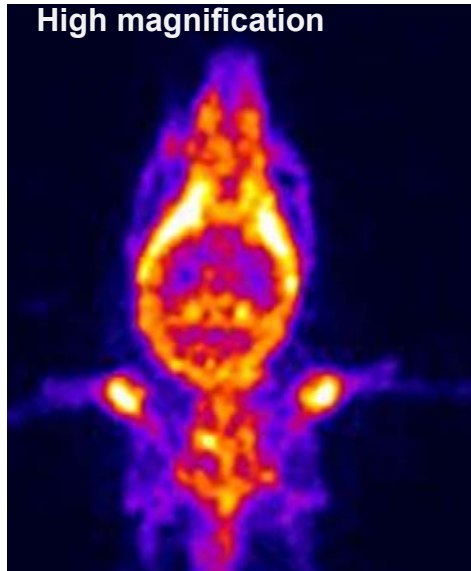
10x20 cm² NaI(Tl) 1.2mm pitch pixellated modular detector



Parallel Hole Collimator



Pinhole Collimator



Courtesy of JHU
Maryland, USA
B.M.W.Tsui

INFN Ecorad Collaboration

dual modality imager

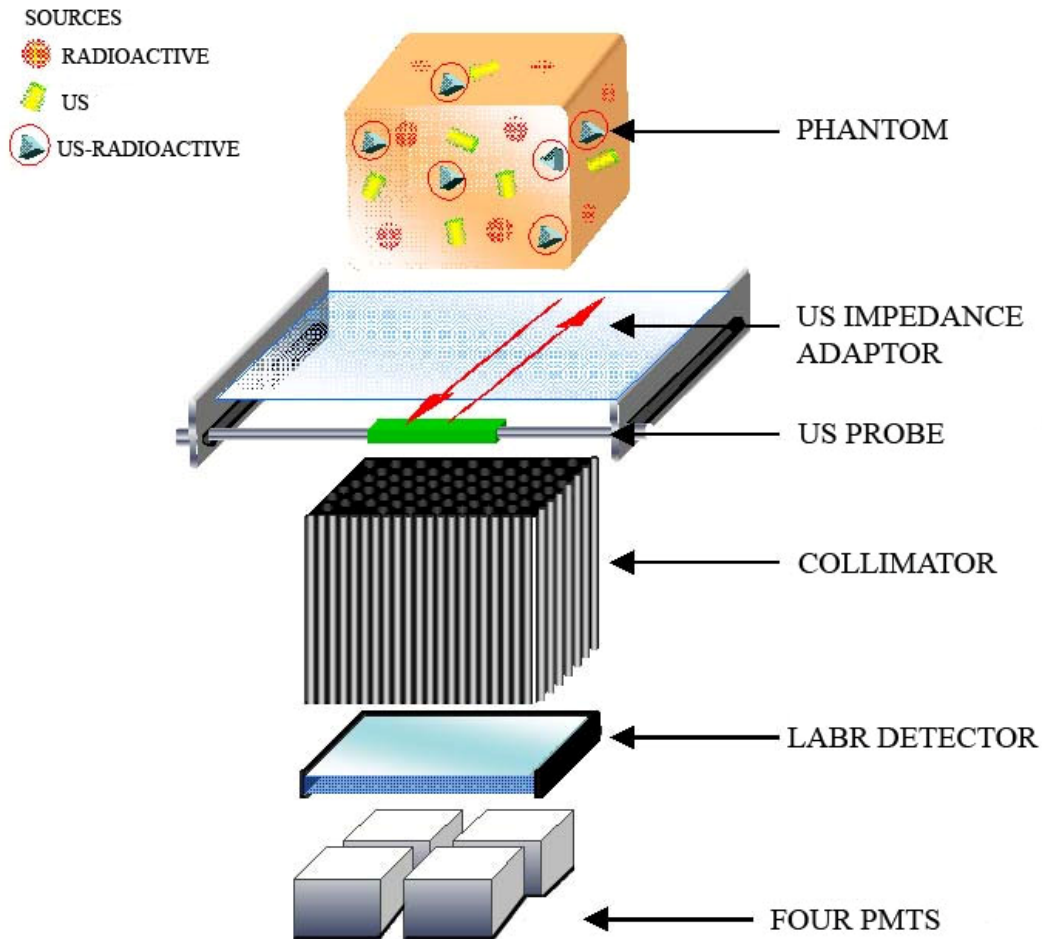
- R. Pani, R.Pellegrini, M.N.Cinti, R. Scaf , **INFN -Roma I.**
- V. Orsolini Cencelli, A. Baroncelli, P. Bennati, E. D'Abramo, F. de Notaristefani, A. Fabbri, D. Sacco, **INFN - Roma III .**
- F. Navarra, G. Baldazzi, N. Lanconelli, S Lo Meo, A. Perrotta, **INFN – Bologna.**
- G. Moschini, G. Boccaccio, P. Rossi, M. Bello, **INFN - Laboratori Nazionali di Legnaro.**

- ❖ The ECORAD collaboration aims to develop a dual compact camera for acquiring ultrasound and scintigraphic images.
- ❖ It will allow to get both morphological and functional information on the same device. A volumetric image containing the fusion information will be provided to the user

Ecorad Experiment Motivations

- Small FoV gamma cameras improve visual quality by a closer positioning to the object
- Radionuclide imaging intrinsically lacks anatomic cues that are needed to localize or stage disease and typically has poorer statistical and spatial characteristics than anatomic imaging methods.
- Functional and anatomic information need to be considered together if one wants to give meaning to a small photon emission image and obtain a more reliable diagnosis.
- Ultrasounds are a cost-effective and reliable method.
- Ultrasound probes are one of the most common ways to assemble portable devices.

ECORAD dual modality imager



Application field:

- Core biopsy
- Lymphnode scintigraphy
- Breast scintigraphy
- Intraoperative probe

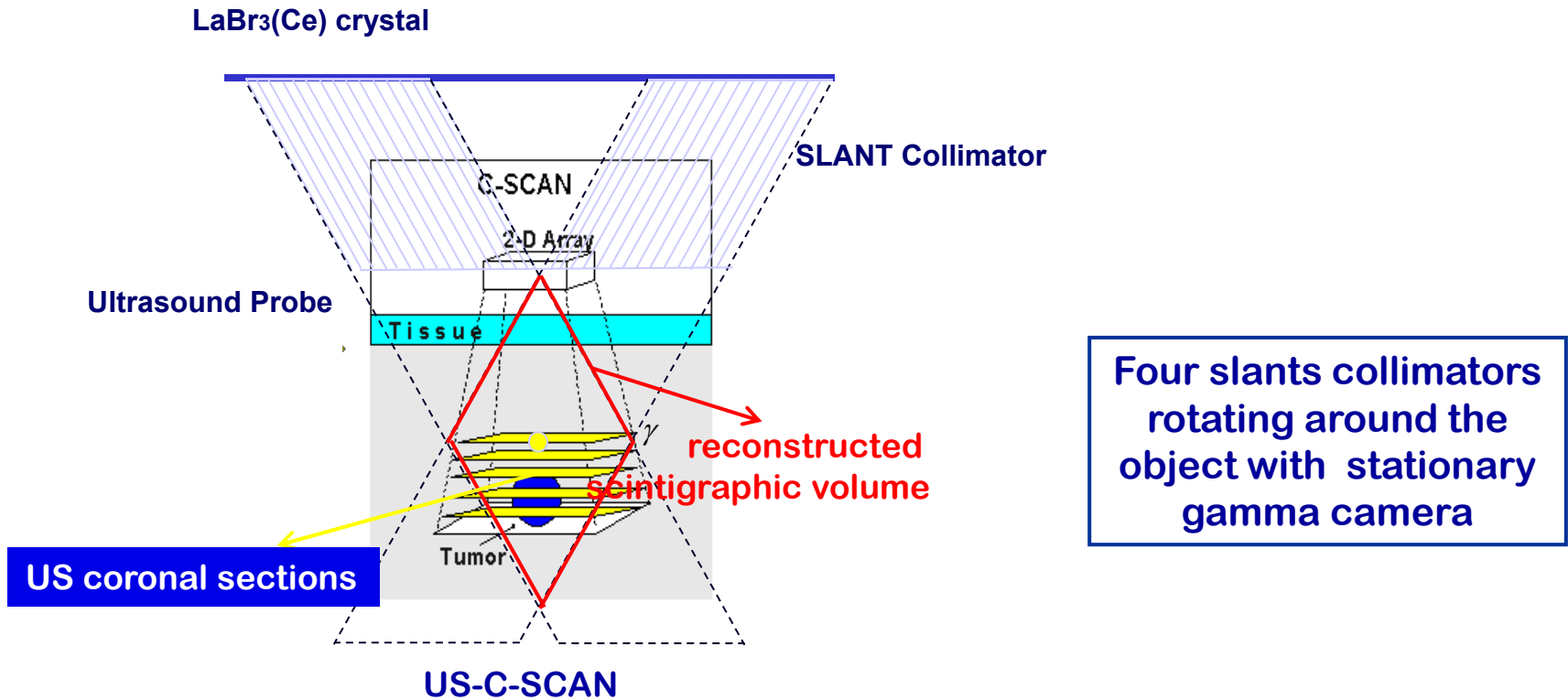
Dual modality system for functional and morphological imaging

Gamma camera based on $\text{LaBr}_3:\text{Ce}$ scintillator integrated with US linear transducer

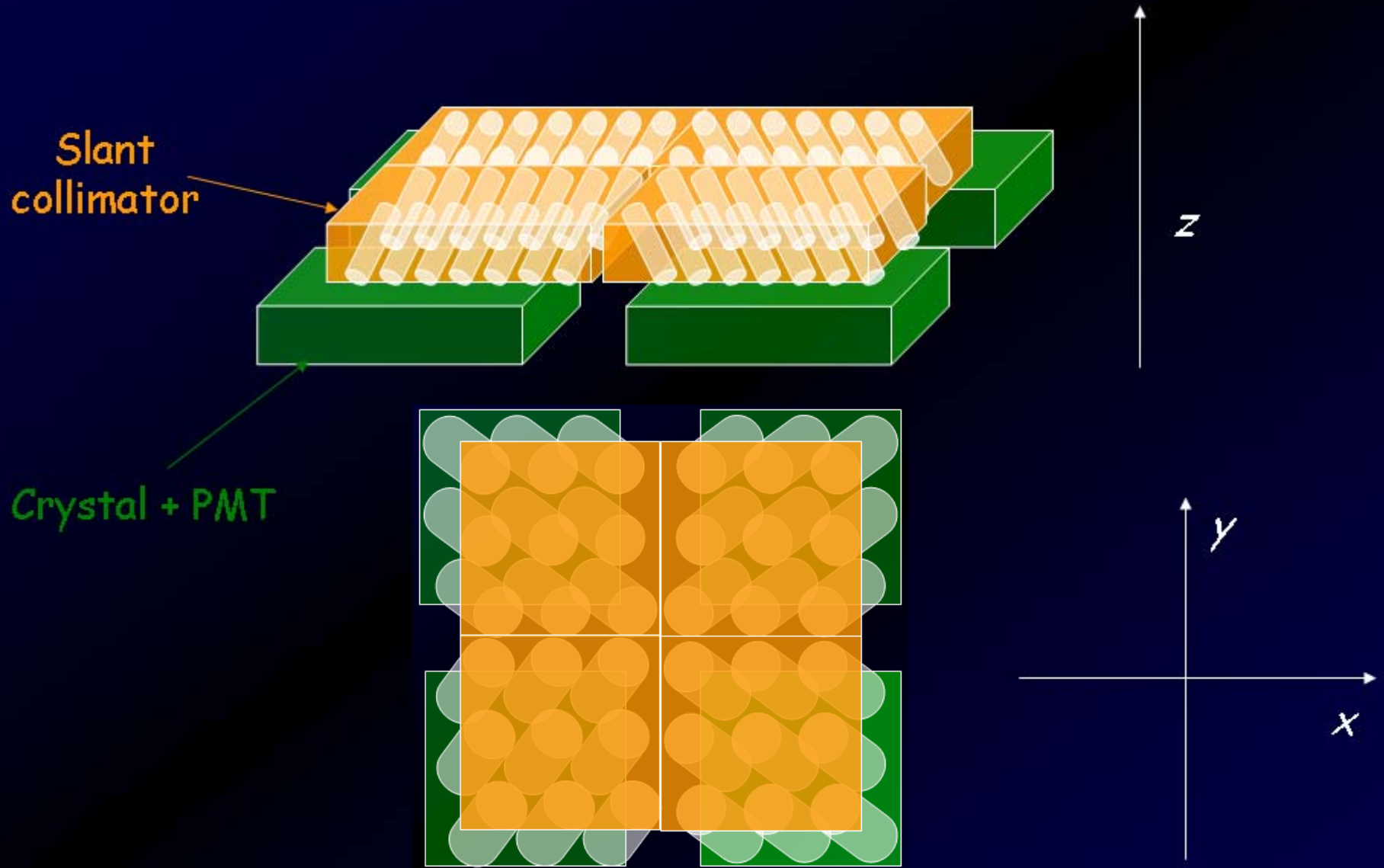
ECORAD dual modality imager

Integrated system for morphological and functional imaging

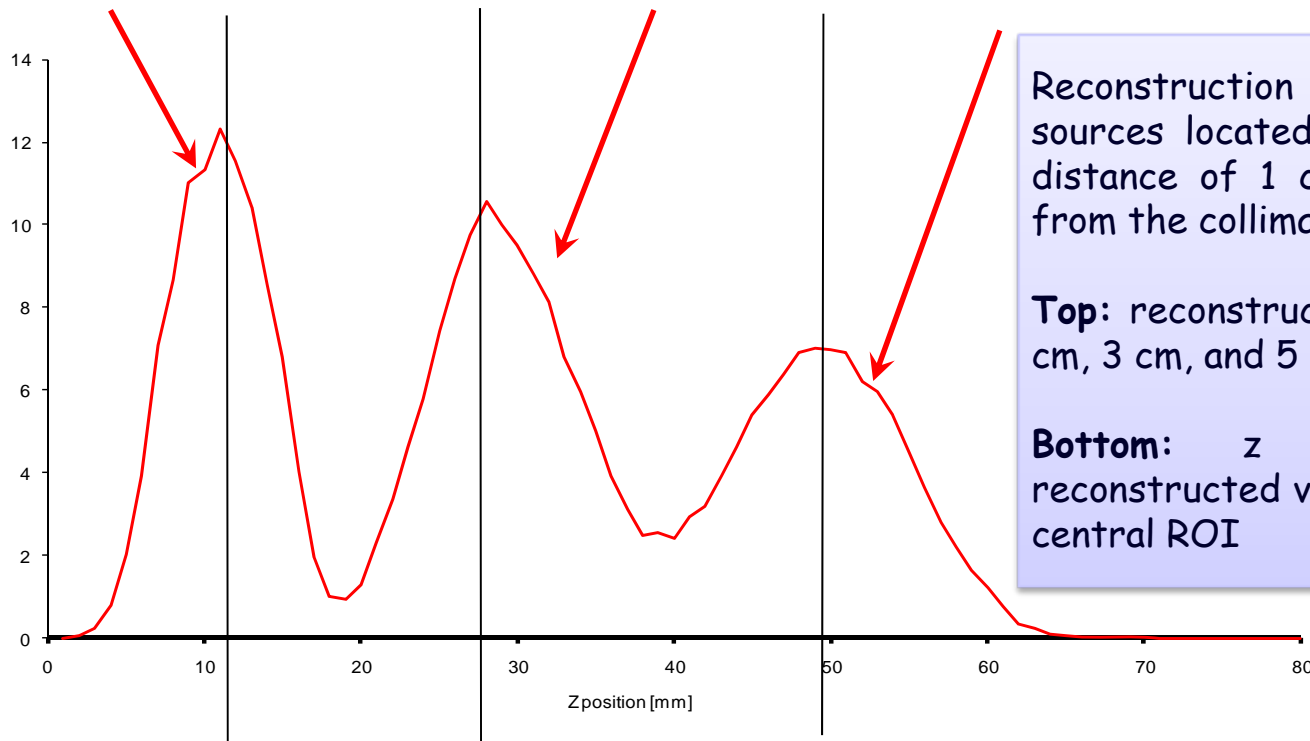
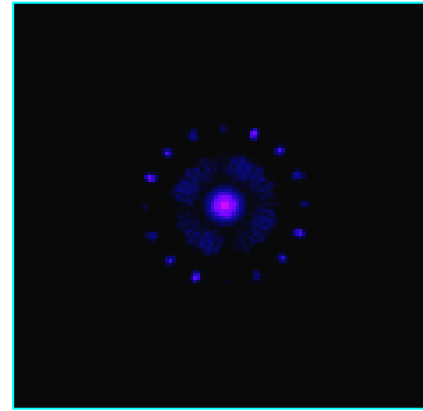
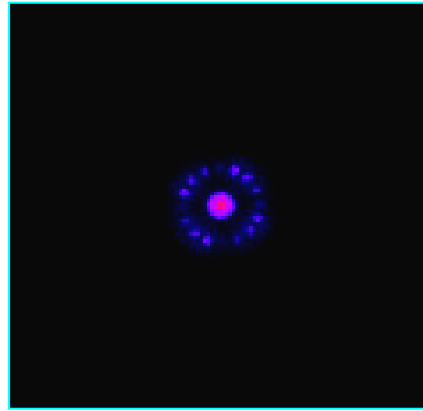
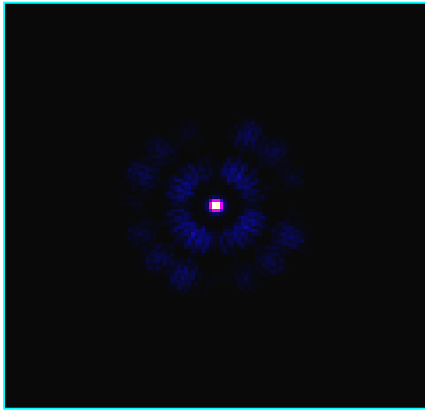
Images reconstruction geometry gamma and 3D US



Sketch of the slant collimators



Point Sources



Reconstruction of three point sources located on the z axis at a distance of 1 cm, 3 cm, and 5 cm from the collimator.

Top: reconstructed slices at depth 1 cm, 3 cm, and 5 cm.

Bottom: z profile of the reconstructed volume estimated on a central ROI

“Biological” Experiment

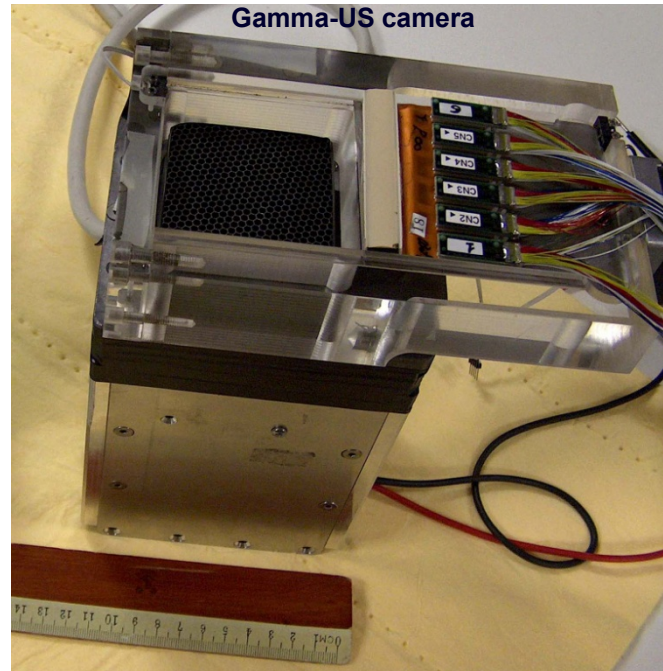


Quail egg

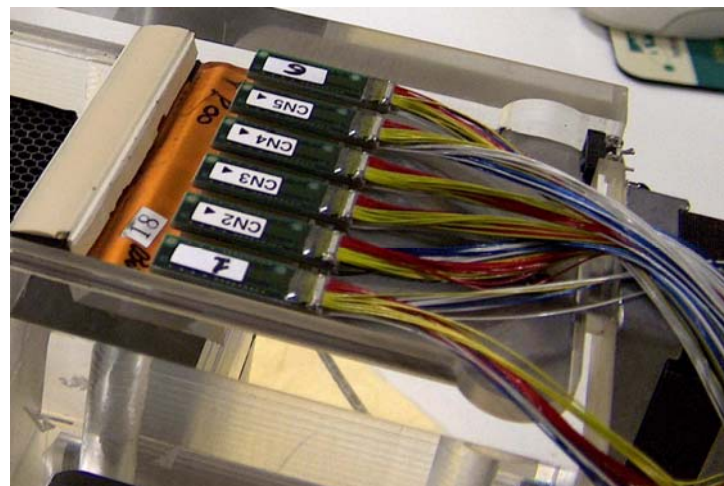
Phantom



Front view

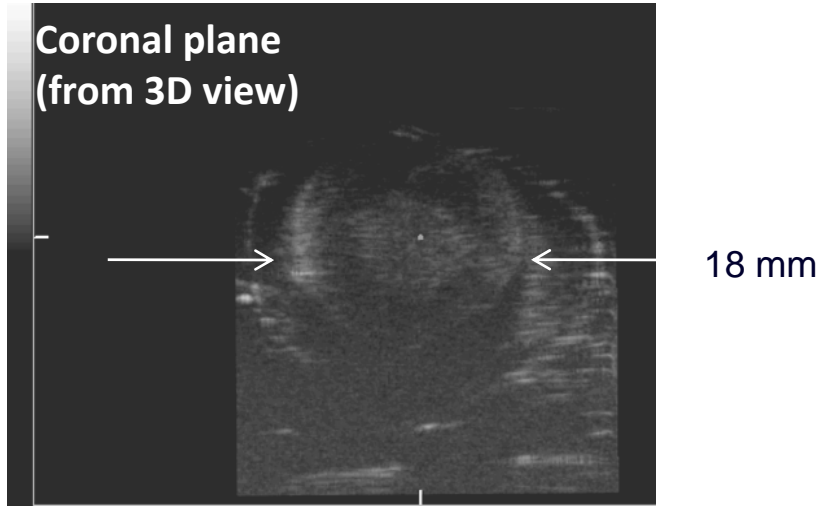
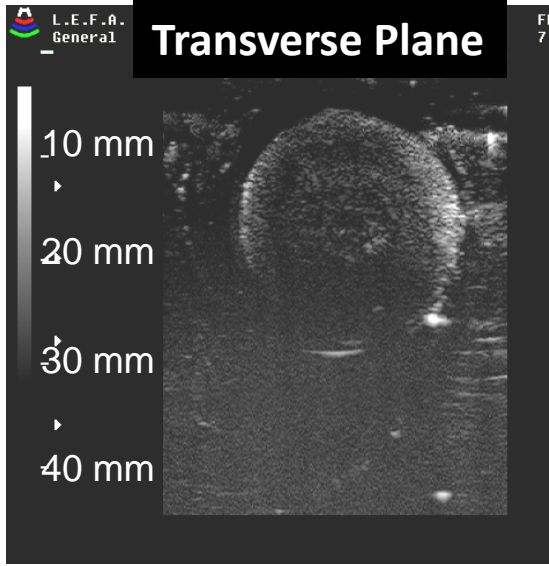
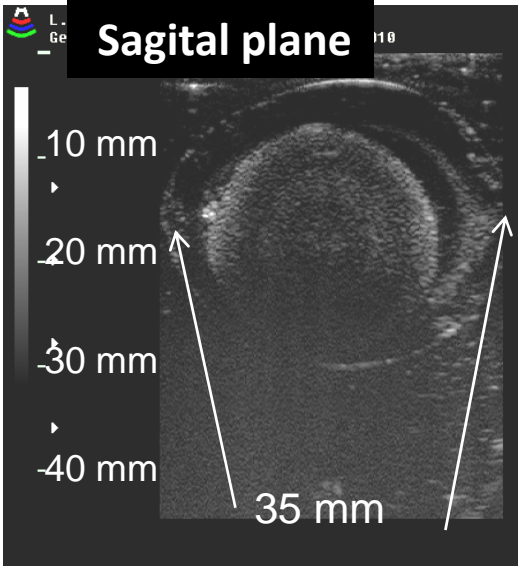
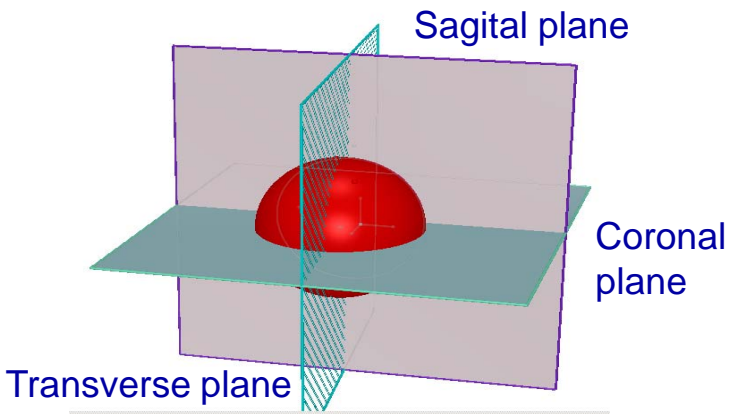


Small FoV
gamma camera



US probe

3D Ultrasound – imaging (35 mm probe – 10MHz)

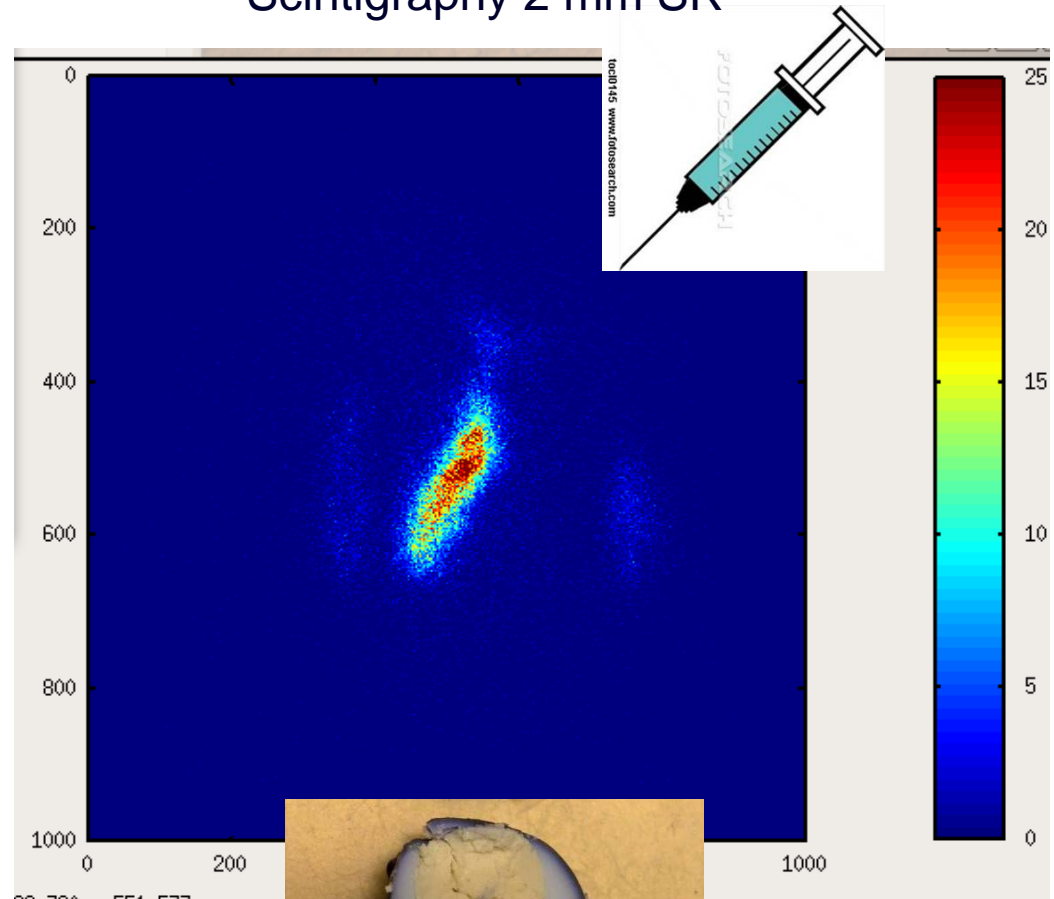


US and Scintigraphic images : 3D US & 2D Gamma

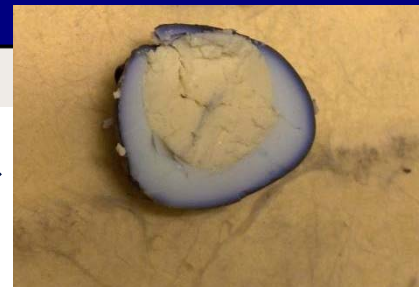
US Image 1mm SR



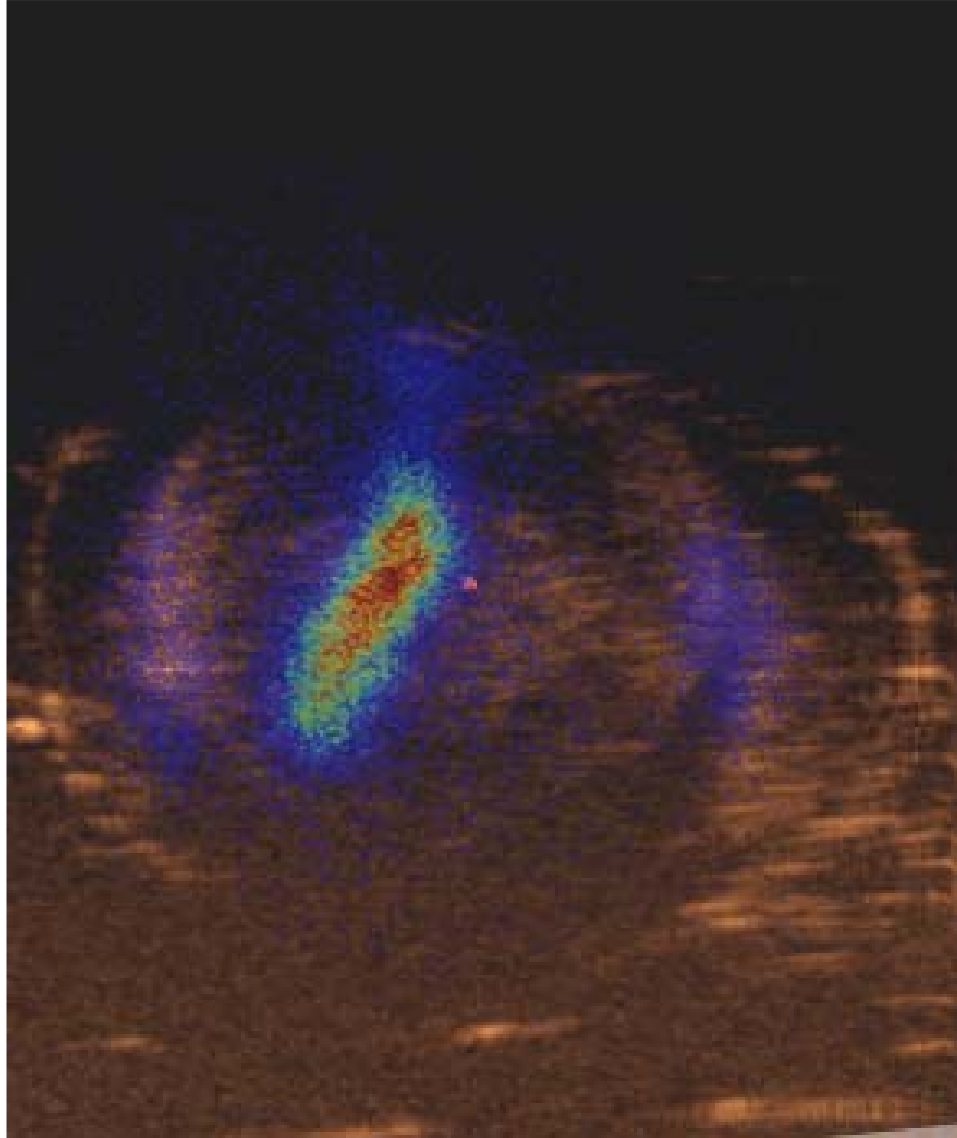
Scintigraphy 2 mm SR



Egg after injection
(20 μ l Tc99m + methylene blue



*US-Scintigraphy dual image:
3D US & 2D Gamma*



Conclusioni

Sfide future in SPET

- ✓ Cristalli continui e nuova matematica della posizione : alta risoluzione spaziale, alta risoluzione energetica, minimo numero di catene elettroniche di lettura ,basso costo.
- ✓ Camere ad alta risoluzione spaziale intrinseca con acquisizioni combinate con collimatori paralleli e pinhole per esperimenti biologici
- ✓ Gamma Camere di piccolo campo combinate con sistemi di imaging anatomico (dual imaging)
- ✓ Gamma camere o rivelatori da utilizzare con sonde intracavitarie e/o laparoscopiche
- ✓ Nuovi metodi di ricostruzione tomografica basati su camere statiche e collimatori paralleli obliqui ad angolo variabile